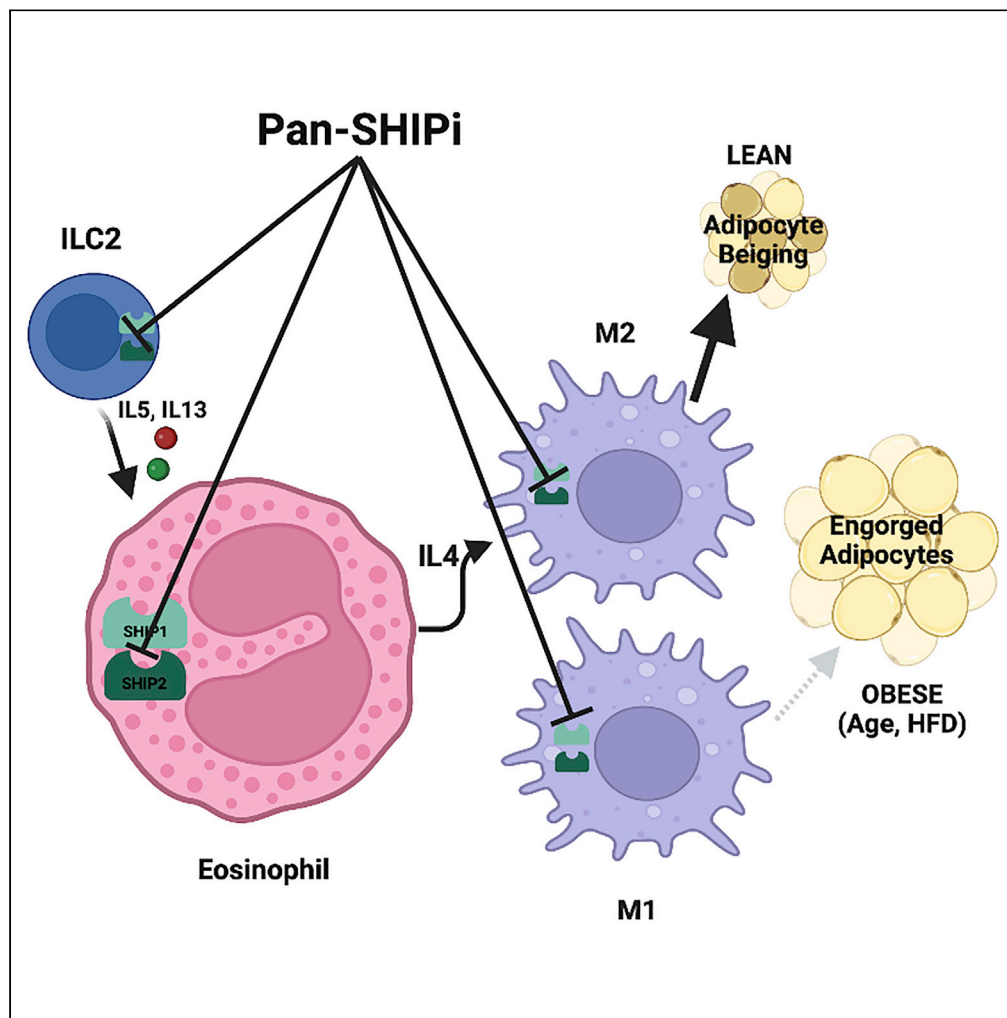**Article**

Obesity control by SHIP inhibition requires pan-paralog inhibition and an intact eosinophil compartment

Sandra Fernandes,
Neetu Srivastava,
Chiara Pedicone,
..., Benedict J.
Chambers, John
D. Chisholm,
William G. Kerr

wgkerr@mac.com

Highlights

Pan-SHIP1/2 inhibitors (pan-SHIPi) reverse diet-induced obesity and hyperglycemia

Prevention of diet-induced obesity (DIO) by pan-SHIPi requires eosinophils

Genetic inactivation of both SHIP1 and SHIP2 in immune cells reduces DIO

Pan-SHIPi reduces obesity and enhances adipose ILC2 cell function in aged hosts

Article

Obesity control by SHIP inhibition requires pan-paralog inhibition and an intact eosinophil compartment

Sandra Fernandes,[1] Neetu Srivastava,[1] Chiara Pedicone,[1] Raki Sudan,[1] Elizabeth A. Luke,[1] Otto M. Dungan,[2] Angela Pacherille,[2] Shea T. Meyer,[2] Shawn Dormann,[2] Stéphane Schurmans,[3] Benedict J. Chambers,[4] John D. Chisholm,[2,6] and William G. Kerr[1,2,5,6,7,*]

SUMMARY

Here we extend the understanding of how chemical inhibition of SHIP paralogs controls obesity. We compare different classes of SHIP inhibitors and find that selective inhibitors of SHIP1 or SHIP2 are unable to prevent weight gain and body fat accumulation during increased caloric intake. Surprisingly, only pan-SHIP1/2 inhibitors (pan-SHIPi) prevent diet-induced obesity. We confirm that pan-SHIPi is essential by showing that dual treatment with SHIP1 and SHIP2 selective inhibitors reduced adiposity during excess caloric intake. Consistent with this, genetic inactivation of both SHIP paralogs in eosinophils or myeloid cells also reduces obesity and adiposity. In fact, pan-SHIPi requires an eosinophil compartment to prevent diet-induced adiposity, demonstrating that pan-SHIPi acts via an immune mechanism. We also find that pan-SHIPi increases ILC2 cell function in aged, obese mice to reduce their obesity. Finally, we show that pan-SHIPi also reduces hyperglycemia, but not via eosinophils, indicating a separate mechanism for glucose control.

INTRODUCTION

Obesity and its associated metabolic disorders have become a global epidemic affecting millions of people worldwide. It is now appreciated that metabolism and immunity are intertwined as inflammatory macrophages recruited to visceral adipose tissue (VAT) can promote the onset of obesity and insulin resistance.[1–3] In addition, an M1-like macrophage population in VAT has recently been shown to limit the thermogenic capacity of adipocytes through consumption of norepinephrine (NE) produced by sympathetic neurons that innervate VAT.[4–6] A counterbalance to these pro-inflammatory myeloid populations in VAT are immunoregulatory myeloid cells, AAM/M2 macrophages and myeloid-derived suppressor cells (MDSC).[1,7–12] Treg cells can also oppose inflammatory stressors on adipocytes and thus promote improved control of blood glucose levels, although they do not reduce adiposity.[8,13,14] Innate lymphocyte type 2 (ILC2) cells present in the VAT can, via production of the type-2 cytokines IL-5 and IL-13, promote increased numbers of eosinophils. IL-4 producing eosinophils are then able to bias myeloid differentiation in the VAT toward immunoregulatory AAM/M2 cells to promote leanness and improve blood glucose control.[15–18] In this mechanism of immune control of obesity, M2 macrophages may express tyrosine hydroxylase (TH) to enable their production of NE that promotes UCP1 expression and thermogenesis by adipocytes.[16] This adrenergic function of M2/AAM cells has recently been challenged,[19] although others have independently replicated that M2/AAM cells are capable of induced TH expression at the mRNA and protein level.[20]

The family of SH2-containing inositol phosphatases consists of only two paralogs, SHIP1 (*INPP5D*) and SHIP2 (*INPPL1*). SHIP1 and SHIP2 are currently thought to have largely distinct functions *in vivo* as phenotypes in SHIP1$^{-/-}$ mice are primarily hematologic[21–23] or immunological,[24–29] and consequently life-threatening. Conversely, SHIP2$^{-/-}$ mice are viable and lack demonstrable hematolymphoid abnormalities. Intriguingly, SHIP2$^{-/-}$ mice are resistant to obesity following consumption of a high-fat diet (HFD).[30] However, the cellular and molecular basis for this resistance has not been defined, and could perhaps be immune-mediated as SHIP2 is expressed in both hematopoietic and parenchymal tissues. A small molecule selective inhibitor of SHIP2 has been described and consequently has shown efficacy in murine models

[1]Department of Microbiology & Immunology, SUNY Upstate Medical University, Syracuse, NY, USA

[2]Department of Chemistry, Syracuse University, Syracuse, NY, USA

[3]GIGA Research Centre, Université de Liège, Liège, Belgium

[4]Center for Infectious Medicine, Department of Medicine, Karolinska Institute, Stockholm, Sweden

[5]Department of Pediatrics, SUNY Upstate Medical University, Syracuse, NY, USA

[6]These authors contributed equally

[7]Lead contact

*Correspondence:
wgkerr@mac.com

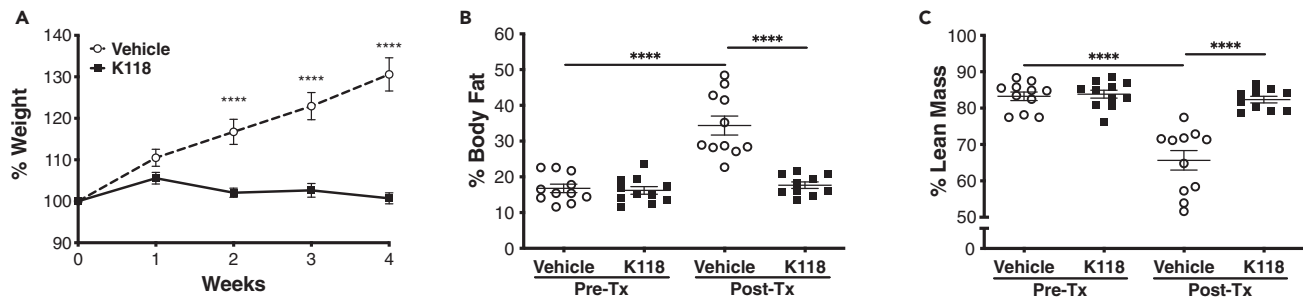https://doi.org/10.1016/j.isci.2023.106071

Figure 1. The pan-SHIP1/2 inhibitor K118 prevents the onset of obesity

(A) Percent body weight, (B) percent body fat and (C) percent lean mass measurements on C57BL/6 mice following *ad libitum* consumption of HFD and simultaneous treatment with K118 or vehicle (H$_2$O). Mice were dosed with K118 two times per week (on days 1 and 4 of each week at 10mg/kg via i.p. injection) for the 4-week duration of the study. Body Fat and Lean mass were measured by DEXA imaging before initiation of the study and after 4 weeks on HFD (Mean ± SEM, 2-way Repeated measures ANOVA with Bonferroni multiple comparison test in A, two-tailed t-test with Welch's correction where needed for B and C, ****$p < 0.0001$, pooled from two experiments with n = 10).

of diabetes and Alzheimer's disease where it improved blood glucose control[31] or cognition,[32] respectively. A variety of small molecule inhibitors of SHIP1 and both SHIP1 and SHIP2 (pan-SHIP1/2 inhibitors) have been described and been shown to enable targeting of SHIP1 or both paralogs *in vivo* – with evidence of therapeutic efficacy in pre-clinical models of diseases that including cancer,[33,34] bone marrow transplantation,[35] blood cell recovery,[36,37] cancer immunotherapy,[38] lethal fungal infection[39] and microglial uptake of β-amyloid in the CNS.[40] Thus, both SHIP1 and SHIP2 have proven to be tractable targets *in vivo* whose selective or dual inhibition has potent physiological effects that can abrogate disease without significant toxicity.[41]

The demonstration that the SHIP inhibitor K118 can reverse obesity following consumption of a HFD,[42] suggested that further analysis of how SHIP inhibition mediates obesity control was merited. In addition, our recent analysis of SHIP inhibitors in tumor immunity showed that compounds with modest selectivity for SHIP1, but which also target SHIP2, like K118, can have distinct activity as compared to more selective SHIP1 inhibitors such as 3AC.[38] For example our recent analysis of a broad panel of SHIP inhibitors showed that pan-SHIP1/2 inhibitors were optimal for promoting homeostatic functions of microglia *in vitro* and *in vivo*, including phagocytosis of Aβ42, the primary constituent of amyloid plaques present in Alzheimer's disease.[40] Using a similar approach here we use both chemical and genetic approaches to dissect whether SHIP1, SHIP2 or both should be targeted in order to control obesity and blood glucose in the context of excess caloric intake. These approaches revealed that pan-SHIP1/2 inhibitors are required for effective obesity control and that eosinophils are essential for this anti-obesity activity, but not for control of blood glucose levels by pan-SHIP1/2 inhibitors.

RESULTS

The pan-SHIP1/2 inhibitor K118 protects mice from HFD-induced obesity

Previously we found that that K118 was effective at reversing obesity in a treatment setting after mice had already become obese due to consumption of high-fat diet (HFD) over a 2 month period.[42] We subsequently found that K118 has only modest selectivity for SHIP1 and consequently inhibits both SHIP1 and SHIP2 with significant potency.[38,40] This led us to question whether solely targeting SHIP1 was required for obesity control. In order to test different classes of SHIP paralog inhibitors for their capacity to reduce obesity, we utilized a prevention model in which mice are placed on HFD while simultaneously being treated with a candidate SHIP inhibitor (SHIPi). To confirm that SHIPi was effective in this prevention model, we introduced mice to HFD consumption and then initiated K118 treatment (2X/week, 10 mg/kg) the same week that mice were placed on HFD. The same K118 dosing regimen that was utilized in the obesity treatment study.[42] We found that K118 treatment in the setting of obesity prevention also protected adult mice from significant weight gain (Figure 1A) and, importantly, also prevented increased adiposity (percent body fat) despite *ad libitum* consumption of HFD over a 4 week period (Figure 1B). Importantly we did not observe wasting in the mice due to K118 treatment as their percent lean mass was maintained as compared to percent lean mass at initiation of HFD consumption (Figure 1C). As expected, vehicle treated mice gained significant body weight and increased their percent body fat and decreased their percent lean
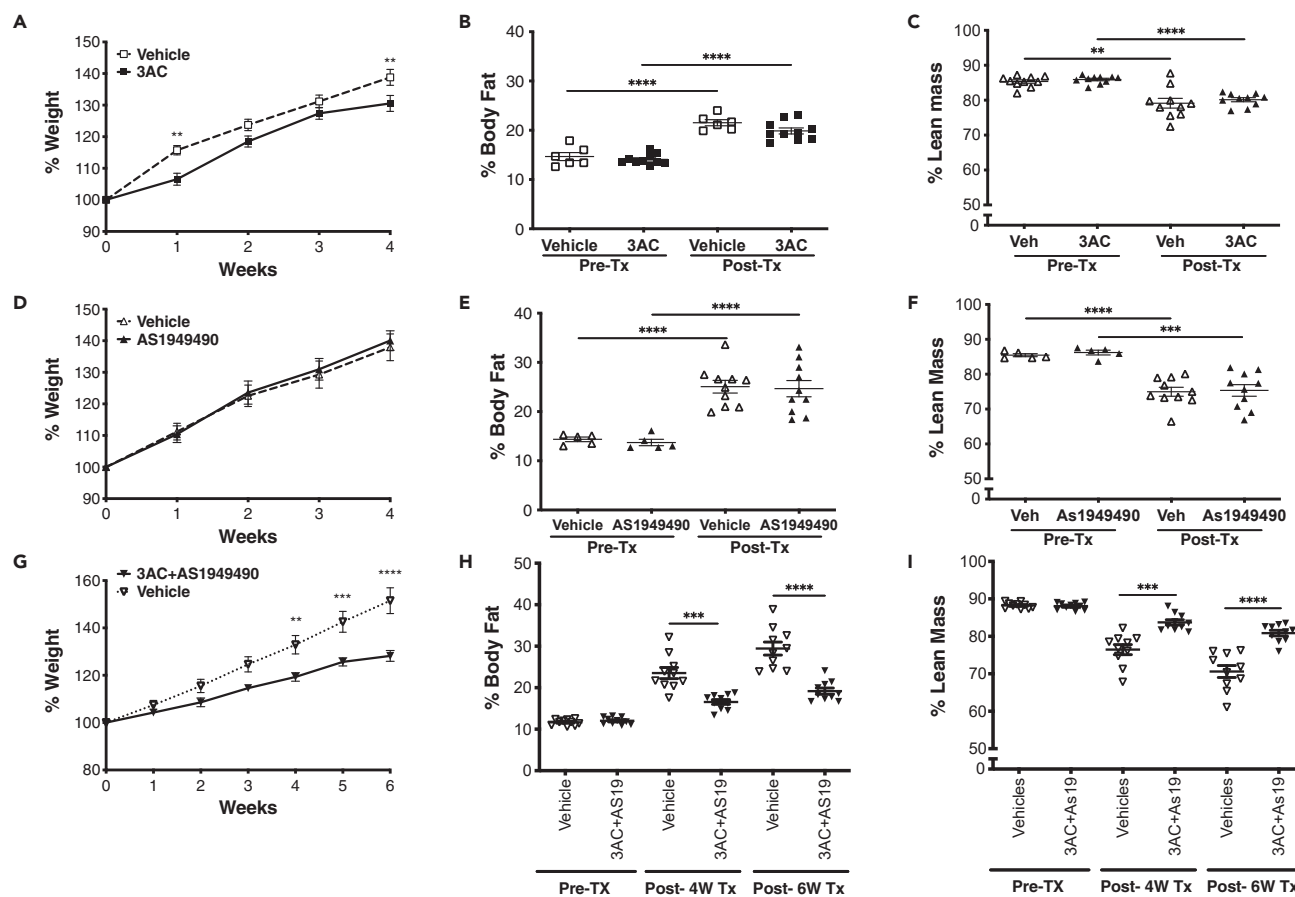
Figure 2. SHIP paralog-selective inhibitors are unable to prevent obesity, but dual treatment with SHIP1- and SHIP2-selective inhibitors reduces weight and body fat increases due to increased caloric intake

(A, D, G) Percent body weight, (B, E, H) percent body fat and (C, F, I) percent lean mass in C57BL/6 mice during HFD consumption and simultaneous treatment with (A–C) 3AC or vehicle (0.3% Klucel:saline), (D-F) AS1949490 or vehicle (5% DMSO:saline) or (G–I) dual treatment with both 3AC and AS1949490 (As19) or dual vehicle (0.3% Klucel:saline + 5% DMSO:saline). Mice were dosed with 3AC and/or AS1949490 or vehicle two times per week (on days 1 and 4 of each week at 26.5mg/kg for 3AC or 20mg/kg for AS1949490 via i.p. injection) for the 4-week duration of the study. (Body Fat and Lean mass were measured by DEXA imaging before initiation of the study and after 4 or 6 weeks on HFD with SHIPi or vehicle treatment (Mean $\pm$ SEM, 2-way repeated measures ANOVA with Bonferroni multiple comparison test in A, B, D, G, two-tailed t-test with Welch's correction when needed for C, E, F, H, and I, **$p < 0.01$, ***$p < 0.001$,****$p < 0.0001$, pooled from two experiments with n = 5).

mass following initiation of HFD consumption.(Figures 1A–1C) Consistent with its ability to reverse obesity in a treatment setting,[42] these findings show that the pan-SHIP1/2 inhibitor K118 is also able to prevent obesity during consumption of a HFD and confirmed that this model could be used to assess the effectiveness of SHIPi strategies in diet-induced obesity.

Paralog-selective SHIP inhibitors are ineffective at prevention of diet-induced obesity

The above findings established that a pan-SHIP1/2 inhibitor could prevent obesity following increased caloric intake. However, this could be due to K118 inhibition of either SHIP1 or SHIP2, and thus unrelated to its ability to inhibit both SHIP paralogs simultaneously. If this were the case, then either SHIP1- or SHIP2-selective inhibition should be able to protect mice from diet-induced weight gain and adiposity. In fact, genetic analysis suggested that solely targeting SHIP2 might enable control of diet-induced obesity.[30] To examine these different possibilities, we treated mice placed on an HFD with either a SHIP1-selective inhibitor (3AC)[36] or SHIP2-selective inhibitor (AS194940),[31] each of which have been found to be effective at targeting SHIP1 or SHIP2 in vivo, respectively.[31,33,36–38,43,44] We found that both the SHIP1-selective inhibitor 3AC (Figures 2A–2C) and the SHIP2-selective inhibitor AS1949490 (Figures 2D–2F) are incapable of preventing body weight gain and increased adiposity (percent body fat), and loss of lean mass upon consumption of an HFD. Mice treated with either compound gained essentially the same amount of weight and

increased body fat to the same degree as their respective vehicle controls. Thus, SHIP paralog selective inhibitors fail to protect from obesity suggests that the capacity of K118 to prevent obesity could be due to its capacity inhibit both SHIP1 and SHIP2 simultaneously.

Dual targeting of SHIP1 and SHIP2 with paralog-selective inhibitors reduces obesity and loss of lean mass caused by increased caloric intake

We considered then that both SHIP paralogs must be targeted *in vivo* in order to reduce weight gain and increased adiposity during HFD consumption. Thus, we undertook a study where we simultaneously treated mice consuming a HFD with both 3AC and AS1949490. In this setting we found that both vehicle and 3AC + AS1949490 treated groups gained weight while consuming HFD. However, the 3AC + AS1949490 treated group gained significantly less weight at 4 weeks after initiation of HFD. When inhibitor treatment was continued through 6 weeks the difference in body weight became even more apparent (Figure 2G). Importantly, mice co-treated with 3AC + AS1949490 also acquired considerably less body fat than vehicle treated mice as measured at 4 and 6 weeks of HFD consumption, (Figure 2H) and retained a greater proportion of lean mass versus the vehicle control group (Figure 2I). As with body weight, the reduction in body fat was more apparent after the treatment was continued for 6 weeks. Although 3AC + AS1949490 treatment does provide a significant degree of protection from diet-induced obesity this protection is not as complete as we observed with K118 (Figure 1). The reason for this is not clear, but one possibility is that K118 has greater potency against SHIP1 than 3AC, and thus more effectively targets both SHIP paralogs than the combination of 3AC and AS1949490. Taken together these findings demonstrate that significant control of diet-induced obesity is achieved by simultaneous inhibition of both SHIP paralogs, and not by paralog selective SHIP inhibition.

Other pan-SHIP1/2 inhibitory compounds also reduce diet-induced obesity

To further test and validate the hypothesis that pan-SHIP1/2 inhibition is necessary for effective obesity control we sought to test other pan-SHIP1/2 inhibitors we have recently identified.[40,41] These include compounds of a completely different chemical class than aminosteroids such as the tryptamine K149,[34,39,46] but also a water soluble aminosteroid K161 that has significant bioavailability *in vivo*, including the ability to cross the blood brain barrier to access brain-resident microglia.[40] Although the capacity of K149 and K161 to inhibit recombinant SHIP1 and SHIP2 enzyme activity *in vitro* has previously been established,[41,45] including several different tryptamine analogs of K103 that include K149,[46] we have recently found that K149 and K161 can inhibit SHIP1 in cells based on their ability to potently induce G-CSF in mice (data not shown). Thus, treatment with K149 or K161 phenocopies a unique genetic phenotype exhibited by SHIP1 KO mice, that is also observed in WT mice treated with either the SHIP1-selective inhibitor 3AC or the pan-SHIP1/2 inhibitor K118.[37] In addition, both K149 and K161 reduce the basal Akt phosphorylation at Ser473 and phosphorylation of its downstream target mTOR in C2 BV2 cells that have been gene edited to only express the SHIP2 paralog[40] (Figure S1). The SHIP1/2 product $PI(3,4)P_2$ is essential for Akt phosphorylation at Ser473 and moreover promotes Akt activity.[47–49] These studies provide additional confirmation that K149 and K161 are capable of targeting both SHIP paralogs in cells. We then tested the utility of these pan-SHIP1/2 inhibitors as potential therapeutics for obesity control. We initially examined whether K149 could also prevent or reverse obesity caused by consumption of a HFD (Figure 3). As with the aminosteroid K118, the tryptamine K149 significantly reduced weight gain during a 6-week period of HFD consumption (Figure 3A). This was evident in the K149-treated mice as they exhibited only a negligible increase in percent body fat, whereas vehicle treated mice gained significantly more body fat than their K149-treated counterparts (Figure 3B). Importantly, K149 treated mice on HFD maintained the same percent lean mass as they had before starting on HFD, (Figure 3C) indicating K149 does not promote weight control through adverse effects on physiology that promote wasting. We also found that K149 can protect mice in a treatment model of HFD induced obesity. In this setting, mice were first rendered obese by consumption of HFD for 2 months after which they were treated with K149 or vehicle (2X per week) whilst continuing to consume HFD. We found that K149 significantly decreased both body weight (Figure 3D) and percent body fat (Figure 3E) within 4 weeks of treatment despite continued HFD consumption. Importantly, K149 treatment increased percent lean mass (Figure 3F) in the obese mice indicating weight loss was not due to wasting. We also found that the pan-SHIP1/2 inhibitory aminosteroid K161[40] also protects mice from weight gain and obesity in a prevention setting, (Figures 4A–4C) but also when used to treat mice that are presently obese and continue to consume a HFD diet (Figures 4D–4F). Thus, three pan-SHIP1/2 inhibitory compounds (K118, K149, K161) derived from two different chemical classes (aminosteroids and tryptamines) have a potent capacity to mediate obesity control in the context of excess
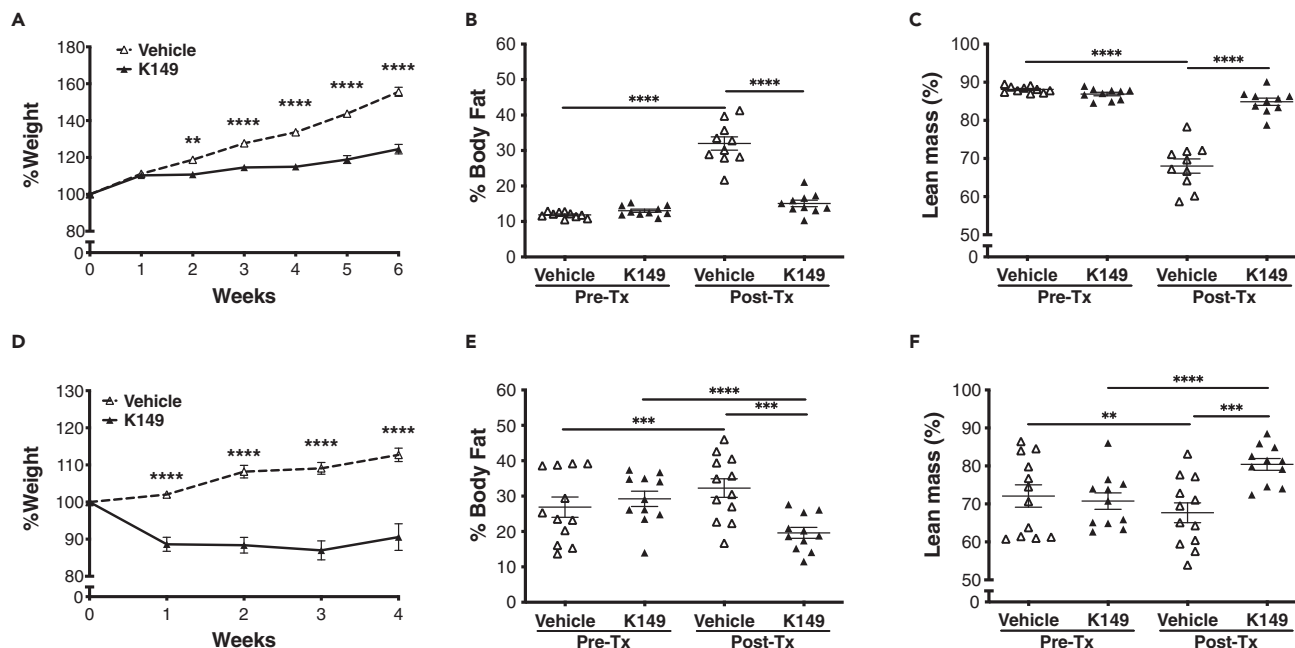
Figure 3. The pan-SHIP1/2 inhibitor K149 prevents the onset and reverses diet-induced obesity

(A, D) Percent body weight, (B, E) percent body fat and (C, F) percent lean mass measurements on C57BL/6 mice following *ad libitum* consumption of an HFD and simultaneous treatment with K149 or vehicle (5% DMSO:saline). Mice were dosed with K149 two times per week (on days 1 and 4 of each week at 10mg/kg via i.p. injection) for the 4–6 weeks duration of the study. Mice in A-C were placed on HFD at the time of the first dose of SHIPi or vehicle, while mice in D-F were placed on HFD for 8 weeks before the start of SHIPi or vehicle and maintained on the diet for the 4 weeks of the study. Body Fat and Lean mass were measured by DEXA imaging before initiation of the treatment and after 4 and 6 weeks on HFD (Mean ± SEM, 2-way repeated measures ANOVA with Bonferroni multiple comparison test in A, D two-tailed t-test for B, C, E and F, **p < 0.01, ***p < 0.001, ****p < 0.0001, each model (prevention or reversal) is pooled from two experiments with n = 5).

caloric intake, while SHIP paralog selective inhibitors like 3AC and AS1949490 are unable to protect from diet-induced obesity.

K149 and K161 pan-SHIP1/2 inhibitory compounds promote increased eosinophil function in the face of HFD stress

The pan-SHIP1/2 inhibitor K118 was found to reduce SHIP1 expression in VAT-resident eosinophils and increase the frequency of IL-4-producing eosinophils in the VAT of obese mice.[42] Thus, we assessed whether the novel pan-SHIP1/2 inhibitors that mediate obesity control or reversal, K149 and K161, can protect the eosinophil compartment and their production of IL-4 during adipogenic stress caused by excess caloric intake. In the setting of obesity prevention, K149 increases the frequency of eosinophils (Figures 5A and 5B, see also Figure S2A), the frequency of eosinophils producing IL-4 versus vehicle controls following 6 weeks of sustained HFD consumption (Figures 5C and 5D), but also increases the amount of IL-4 made on a per cell basis as determined by intracellular staining for IL-4 (Figures 5E and 5F). Consistent with increased IL-4 production by the eosinophil compartment,[10,15,50] the VAT macrophage compartment becomes polarized toward the M2/AAM phenotype (Figures 5G, 5H, and S2B). We then assessed the same VAT immune components in mice rendered obese by HFD consumption, and then treated with the water soluble aminosteroid pan-SHIP1/2 inhibitor K161. K161 treatment also demonstrated a clear capacity to promote VAT eosinophil function in the face of adipogenic stress as K161 increased the frequency of total eosinophils (Figures 6A and 6B), and their absolute numbers per milligram (mg) of epididymal white adipose tissue (eWAT) (Figure 6C). Importantly, eosinophil expression of IL-4 on a per cell basis, (Figures 6D and 6E) and the frequency and absolute number of IL4+ eosinophils was also increased by K161 treatment, (Figures 6F–6H) indicating the macrophage polarizing function of the VAT eosinophil compartment might be augmented by K161, even in the face of HFD-induced adipogenic stress. Indeed, K161 polarized the VAT macrophage compartment toward M2 macrophages, by reducing the number of inflammatory M1-like macrophage per mg of eWAT (Figures 6I-6L). Taken together, these data indicate that pan-SHIP1/2 inhibition has the unique capacity to promote IL4 production at both a cellular (increased
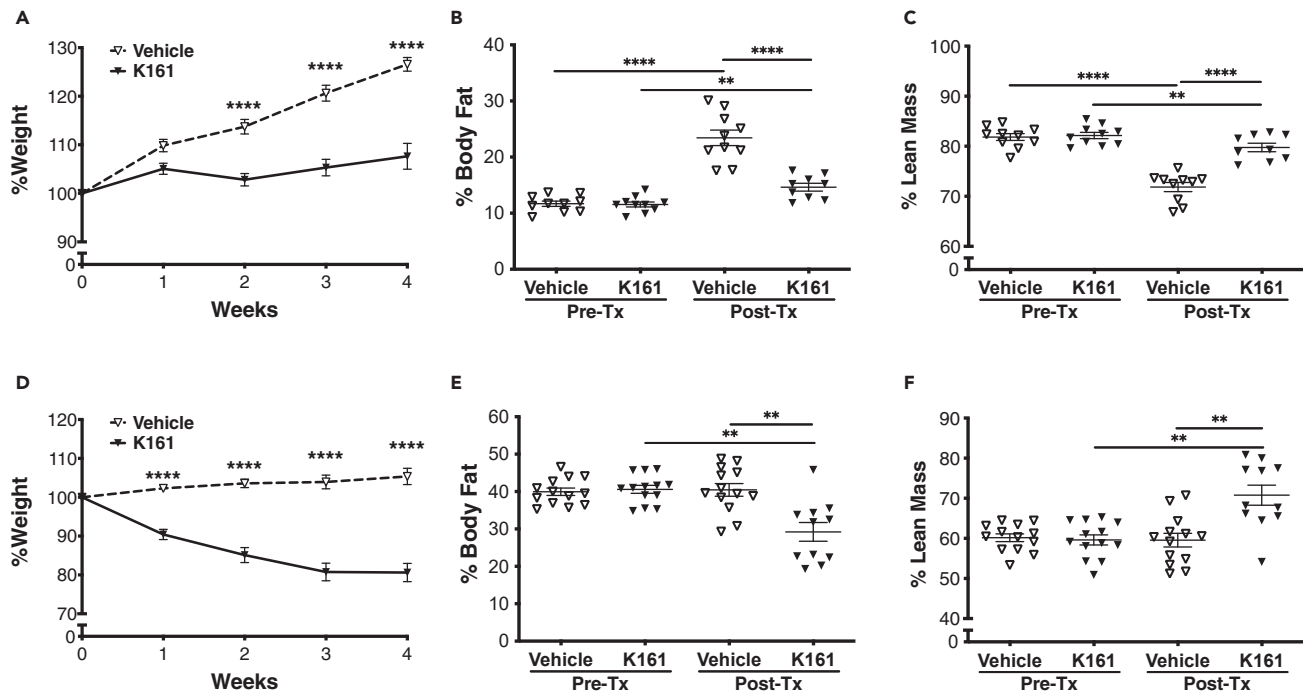
Figure 4. The pan-SHIP1/2 inhibitor K161 prevents the onset and reverses diet-induced obesity

(A, D) Percent body weight, (B, E) percent body fat and (C, F) percent lean mass measurements on C57BL/6 mice following *ad libitum* consumption of an HFD and simultaneous treatment with K161 or vehicle (H$_2$O). Mice were dosed with K161 two times per week (on days 1 and 4 of each week at 10mg/kg via i.p. injection) for the 4-week duration of the studies. Mice in A-C were placed on HFD at the time of the first dose of SHIPi or vehicle, while mice in D-F were placed on HFD for 8 weeks before the start of SHIPi or vehicle and maintained on the diet for the 4 weeks of the study. Body Fat and Lean mass were measured by DEXA imaging before initiation of the treatment and after 4 weeks on HFD (Mean ± SEM, 2-way repeated measures ANOVA with Bonferroni multiple comparison test in A, D, two-tailed t-test for B, C, D and F, **p < 0.01, ****p < 0.0001, each model (prevention or reversal) is pooled from two experiments with n = 5).

number of IL4-expressing cells) and a molecular level (increased IL4 per cell) in the eosinophil compartment that then supports polarization of the VAT macrophage compartment toward an M2 phenotype.

Pan-SHIP1/2 inhibitors are unable to reduce obesity and polarize the macrophage compartment in mice that lack an intact eosinophil compartment

Mice homozygous for the ΔdblGATA mutation lack eosinophils due to a requirement by hematopoietic stem cells for eosinophil lineage commitment promoted by the GATA1 transcription factor.[51] ΔdblGATA mice were subsequently used to show that an eosinophil compartment is required for protection from weight gain and loss of glucose homeostasis following consumption of an HFD.[15,52] Because multiple pan-SHIP1/2 inhibitors promote VAT eosinophil function in different diet-induced obesity settings, we hypothesized that eosinophils might be a critical cellular target of pan-SHIP1/2 inhibitors for obesity control. Thus, we tested the capacity of K118 to mediate obesity control in ΔdblGATA mice and BALB/C mice of the same genetic background. When BALB/C mice, which have an intact eosinophil compartment, were placed on HFD and simultaneously treated with K118 they did not gain body weight to the same degree as vehicle treated controls (Figure 7A). They also showed no increase in percent body fat (Figure 7B) and their lean mass was comparable to that before the initiation of HFD 6 weeks earlier (Figure 7C). As expected, vehicle treated BALB/C mice showed a dramatic increase in percent body fat and loss of lean mass after 6 weeks of HFD consumption (Figure 7C). In the ΔdblGATA mice placed on a HFD, K118 treatment surprisingly did reduce the amount of body weight relative to vehicle treated ΔdblGATA mice placed on a HFD (Figure 7A). However, the K118 treated ΔdblGATA mice increased the percent body fat to the same degree as vehicle treated ΔdblGATA mice, (Figure 7B) indicating eosinophils are required for K118 to prevent a diet-induced increase in adiposity during excess caloric intake. Intriguingly, K118 treated ΔdblGATA mice retained a comparable % lean mass whereas their vehicle treated counterparts lost significant percent of lean body mass (Figure 7C). To provide an independent measure for loss of eosinophil function, as further evidence
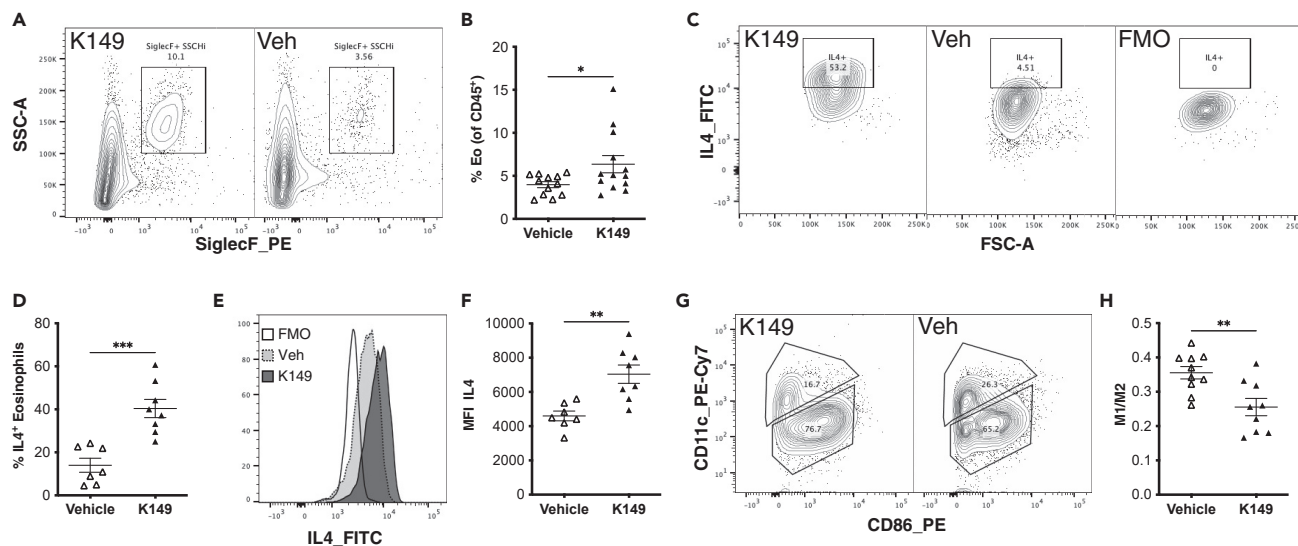
Figure 5. Pan-SHIPi using K149 increases the frequency of IL4-expressing eosinophils and their production of IL4 and promotes M2/AAM polarization

The following data are from an obesity prevention model where K149 treatment was initiated on the same day that mice were placed on HFD for the 6 weeks (A) Representative contour plot for eosinophil gating with the indicated stains (see Figure S2A for additional gating information), (B) frequency of SSC^{Hi}SiglecF$^+$ eosinophils (percent of CD45$^+$), (C) representative contour plot of IL4$^+$ eosinophils (from A), (D) frequency of IL4$^+$ expressing eosinophils and (E) representative flow plot for IL4 median fluorescence intensity (MFI) in all eosinophils (A) with Fluorescence minus control (FMO), (F) total intracellular IL4 was increased in eosinophils isolated from eWAT after treatment with pan-SHIP1/2 inhibitor K149. (G, H) Polarization of macrophages to an M2/AAM phenotype (G, representative gating used to estimate M1 (CD11b$^+$F4/80$^+$Gr1$^-$CD86^{lo}CD11c$^+$) or M2/AAM cells (CD11b$^+$F4/80$^+$Gr1$^-$CD86^{lo}CD11c$^-$) in eWAT after SHIPi treatment (H) M1/M2 ratio calculated as frequency of M1 over frequency of M2 from parent gate (F4/80$^+$Gr1$^-$, see Figure S2B for additional gating information). (Mean ± SEM, one-tailed t-test, *p < 0.05, **p < 0.01, ***p < 0.001, pooled from at least two experiments with n = 5).

that K118 acts on eosinophils *in vivo*, we also assessed M2 macrophage polarization in the vehicle and K118 treated ΔdblGATA mice on HFD. We found that M2/AAM polarization was not induced in ΔdblGATA mice by K118 as compared to vehicle controls (Figure 7D). We then performed a similar study with both K149 and K161. Mice that consumed a HFD for 6 weeks while being treated with K149 (Figure 7E) or K161 (Figure 7I) lost weight as compared to vehicle controls, but did not show a significant decrease in percent body fat (Figures 7F and 7J) or increase in percent lean mass (Figures 7G and 7K) as compared to their respective vehicle control groups following 6 weeks of HFD consumption. In addition, both K149 (Figure 7H) and K161 (Figure 7L) treatment of mice consuming HFD for 6 weeks failed to polarize the VAT M1/M2 compartment toward M2 cells. Thus, all three pan-SHIP1/2 inhibitors, K118, K149, K161, fail to control obesity and polarize the macrophage compartment toward M2 cells in mice that lack an eosinophil compartment during consumption of HFD.

Genetic ablation of both SHIP paralogs in the myelo-eosinophilic compartment promotes reduced body fat

We then sought genetic evidence that both SHIP paralogs should be targeted in the myeloid and/or eosinophil compartments to reduce adiposity during consumption of HFD. Initially we placed the LysMCre driver[53] on SHIP1$^{flox/flox}$, SHIP2$^{flox/flox}$ or SHIP1$^{flox/flox}$SHIP2$^{flox/flox}$ backgrounds. The LysMCre driver has been used by numerous groups for efficient pan-myeloid deletion of floxed genes,[53,54] but has also recently been used to analyze deletion of mTOR in eosinophils,[55] indicating this Cre driver may enable deletion in multiple cell lineages within the myeloid arm of the hematopoietic system. Importantly, we in fact found that there is a partial, but yet significant deletion of SHIP1 protein by flow cytometry in VAT eosinophils using a single cell, intracellular flow assay for SHIP1 expression (Figures 8A–8C). We then placed LysMCre + *flox/flox* mice and their Cre-negative *flox/flox* counterparts on HFD and their body weight and percent body fat was monitored for an 8-week period. During this period body weight was monitored and DEXA measurements were made of percent body fat and lean mass. We found that LysMCre$^+$SHIP1$^{flox/flox}$, LysMCre$^+$SHIP2$^{flox/flox}$ and LysMCre$^+$SHIP1$^{flox/flox}$SHIP2$^{flox/flox}$ gained similar amounts of weight as their SHIP1$^{flox/flox}$SHIP2$^{flox/flox}$ littermate controls. However, the LysMCreSHIP1$^{flox/flox}$SHIP2$^{flox/flox}$ had a significantly lower percent body fat and increased percent lean
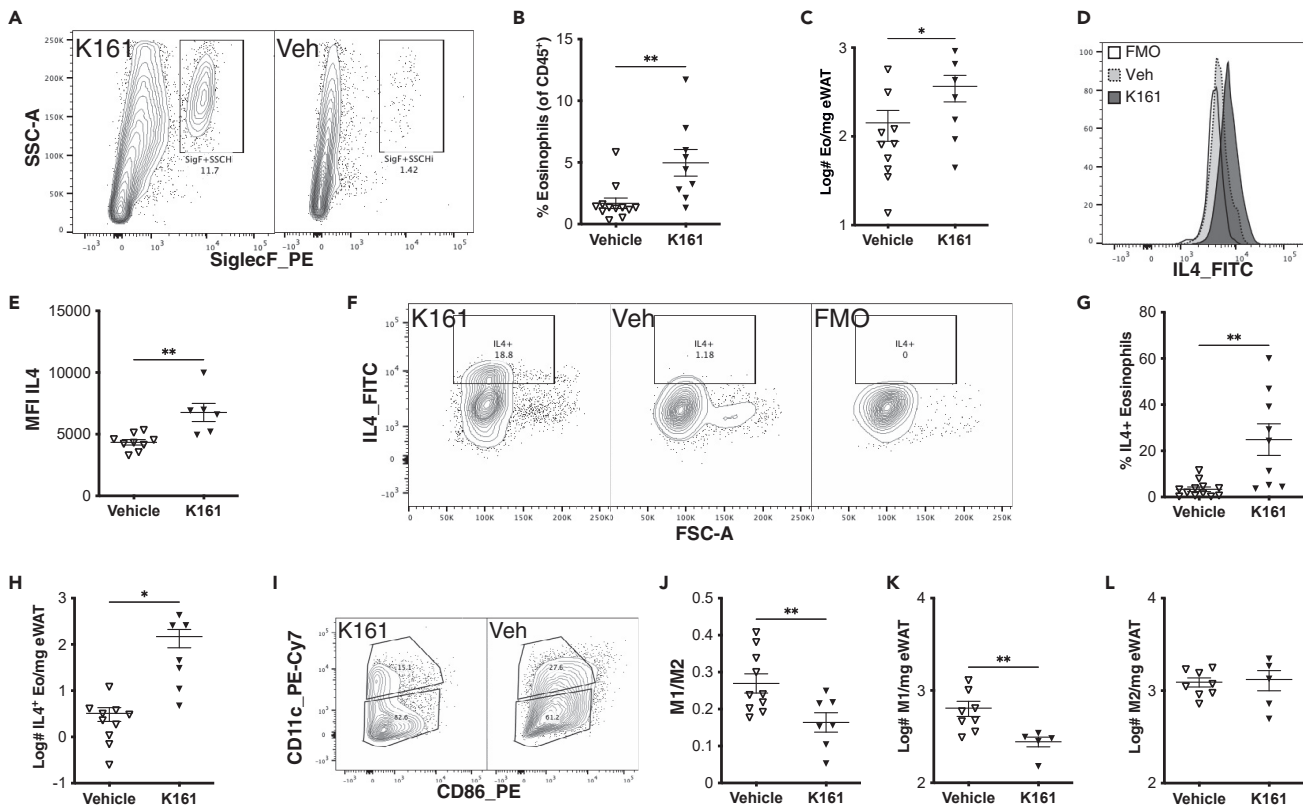
Figure 6. Pan-SHIPi using K161 increases the frequency of IL4-expressing eosinophils and their production of IL4 and promotes M2/AAM polarization

The following data are from an obesity reversal model where mice were place on HFD for 8 weeks before treatment for 4 week with K161. (A) Representative contour plot showing gating to estimate eosinophil numbers and frequency. (B) eosinophil frequency (of CD45$^+$) cells and (C) total number of eosinophils per mg of eWAT (Live, CD45$^+$, SSC^{Hi}SigF$^+$) (D) representative flow plot for IL4 median fluorescence intensity in the eosinophils compartment (A), (E) total intracellular IL4 was increased in eosinophils, (F) representative flow plot for IL4$^+$ eosinophils from total eosinophils (A), (G) IL4$^+$ frequency of total eosinophils and (H) total number of IL4$^+$ eosinophils per mg of eWAT after treatment with pan-SHIP1/2 inhibitor K161. (I-L) Increase polarization of macrophages to an M2/AAM phenotype was observed in eWAT after SHIPi treatment with K161 (I, representative gating of M1 (CD11b$^+$F4/80$^+$CD86^{lo}CD11c$^+$) and M2/AAM cells (CD11b$^+$F4/80$^+$CD86^{lo}CD11c$^-$), (J) Ratio of M1 over M2 cells from parent gate, absolute number of M1 (K) and M2 (L) cells per mg of eWAT. (Mean ± SEM, one-tailed t-test, *p < 0.05, **p < 0.01, pooled from at least two experiments with n = 5, see Figure S2 for gating strategy for Eosinophils and M1 and M2 macrophages).

mass as compared to SHIP1$^{flox/flox}$SHIP2$^{flox/flox}$ littermate controls (Figures 8D and 8E). Neither LysMCreSHIP1$^{flox/flox}$ or LysMCreSHIP2$^{flox/flox}$ mice showed reduced percent body fat or increased percent lean mass versus their respective Cre-negative controls after 8 weeks on HFD (Figure S4), indicating inactivation of both SHIP1 and SHIP2 in myeloid cells and/or eosinophils is needed to reduce adiposity associated with increased caloric consumption. However, no differences was observed in *ad libitum* serum glucose levels between LysMCre$^+$SHIP1$^{flox/flox}$SHIP2$^{flox/flox}$ and their SHIP1$^{flox/flox}$SHIP2$^{flox/flox}$ littermates (Figure S5A). We then performed a similar study, but with a Cre driver (eoCre) that has eosinophil-restricted expression due to homologous recombination of the Cre transgene into the eosinophil peroxidase locus.[56] We confirmed this driver is capable of deletion in VAT eosinophils as we observe efficient ablation of SHIP1 expression in eosinophils using an intracellular flow assay for SHIP1 expression (Figures 8F and 8G). The eoCreSHIP1$^{flox/flox}$, eoCreSHIP2$^{flox/flox}$ and eoCreSHIP1$^{flox/flox}$SHIP2$^{flox/flox}$ cohorts all gained weight while on HFD for 12 weeks to a comparable degree as compared to their corresponding SHIP$^{flox/flox}$ littermate controls. Also, the eoCreSHIP1$^{flox/flox}$ (Figure 8H) and eoCreSHIP2$^{flox/flox}$ (Figure 8I) had inguinal white adipose tissue (iWAT) masses that were a comparable percentage of total body weight as compared to their respective SHIP$^{flox/flox}$ littermate controls (*not significant*(ns), p > 0.05, two-tailed t-test). However, in eoCreSHIP1$^{flox/flox}$SHIP2$^{flox/flox}$ mice inguinal fat pad mass was reduced as a percent of total body weight versus SHIP1$^{flox/flox}$SHIP2$^{flox/flox}$ littermates (Figure 8J). No differences were observed in *ad libitum* glucose between eoCre$^+$SHIP1$^{flox/flox}$SHIP2$^{flox/flox}$ as compared to SHIP1$^{flox/flox}$SHIP2$^{flox/flox}$ littermate controls
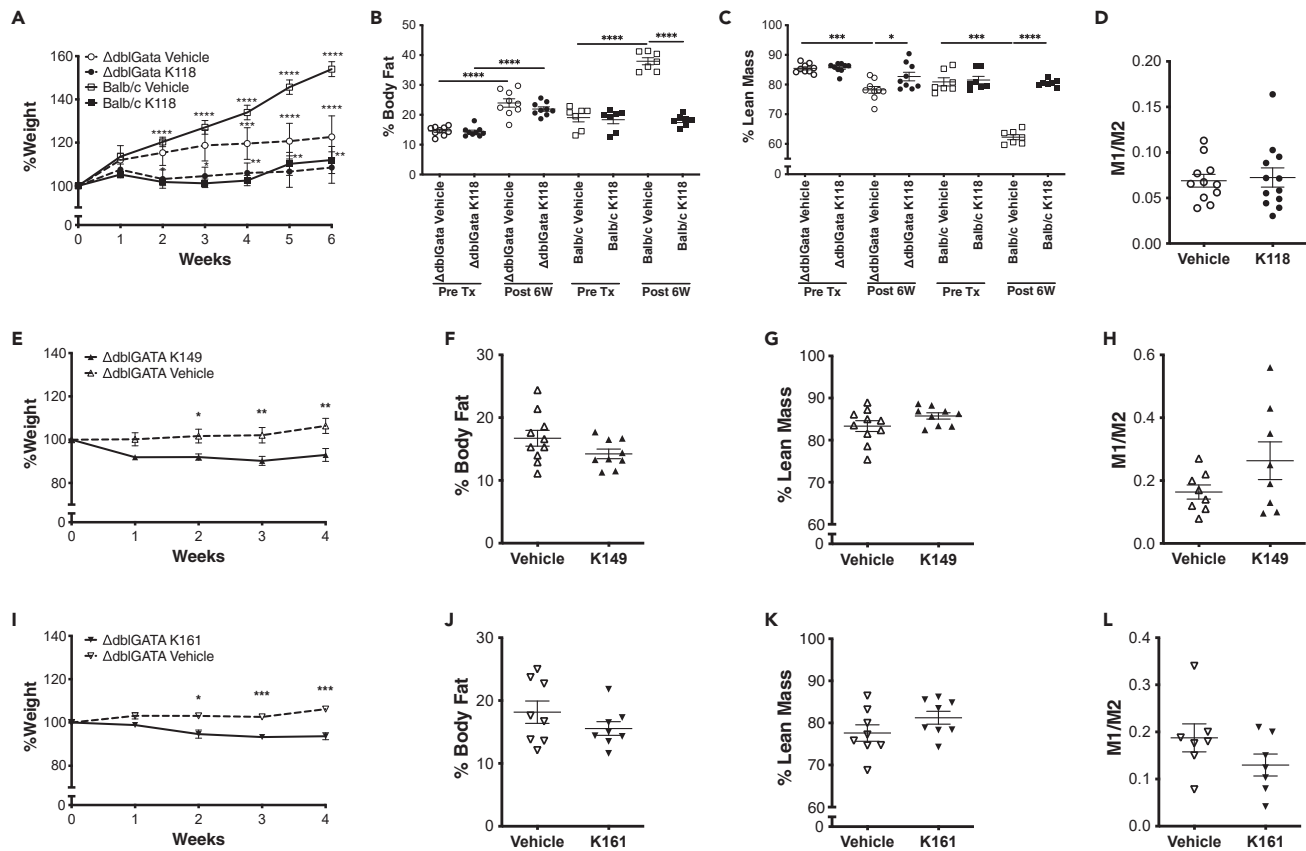
Figure 7. Pan-SHIP1/2 inhibitors limit obesity and promotes M2/AAM polarization via the eosinophil compartment

(A) ΔdblGATA and Balb/c mice were placed on HFD for 6 weeks and simultaneously treated with K118 or vehicle twice a week as described above. Body weight was measured on a weekly basis after initiation of HFD consumption.

(B) The percent body fat and (C) percent lean mass was determined by DEXA imaging of the K118 or Vehicle treatment groups in (A) before (PreTx) and after (Post 6W) 6 weeks of HFD consumption.

(D) eWAT macrophages are not polarized to an M2/AAM phenotype in ΔdblGATA (from mice in A-C) following simultaneous HFD and 6-week treatment of K118, as determined by flow cytometry of eWAT SVC fraction (See gating strategy in Figure S2B and representative flow plots for M1/M2 in Figure S3A). (E-L) ΔdblGATA mice were placed on HFD for 8 weeks before the start of SHIPi or vehicle and maintained on the diet for the 4 weeks of the study. (E, I) Percent body weight, (F, J) percent body fat and (G, K) percent lean mass measurements on ΔdblGATA treated two times per week as above with (E-H) K149 or vehicle (5% DMSO:saline) or (I–L) K161 or vehicle (H$_2$O). Body fat and lean mass were measured by DEXA imaging before initiation of the SHIPi treatment and after 4 weeks on HFD. eWat macrophages are not polarized to an M2/AAM phenotype in ΔdblGATA mice following K149 (H) or K161 (L) treatment as determined by flow cytometry of eWAT SVC fraction as above (See gating strategy in Figure S2B and representative flow plots for M1/M2 in Figures S3B and S3C for K149 and K161, respectively. (Mean ± SEM, 2-way repeated measures ANOVA with Bonferroni multiple comparison test in A, E, I, two-tailed t-test for B-D, F-H, J-L *p < 0.05, **p < 0.01, ***p < 0.001, ****p < 0.0001, each model is pooled from two experiments).

(Figure S5B). Thus, dual SHIP paralog ablation, and not ablation of a single SHIP paralog, exclusively in eosinophils is sufficient to reduce abdominal adiposity associated with HFD consumption. Taken together these genetic studies indicate that both SHIP1 and SHIP2 function in myeloid cells and/or eosinophils could be targeted for obesity control.

ILC2 function is promoted by pan-SHIPi in age-associated obesity

IL5 is a critical driver of eosinophil proliferation, survival and function and ILC2 in the VAT are a crucial local source of this IL5.[17] We previously found that K118 increased serum levels of both IL5 and IL13 in HFD mice.[42] We then examined if this was also the case with more potent and water soluble pan-SHIPi compound K161. We tested this in the context of older mice that only consumed normal chow and exhibited age-associated obesity (>32g body weight, mean 43 ± 6g). We found that twice a week K161 administration to these aged and obese mice led to a ~25% reduction in body weight over a 4-week period as compared to vehicle controls, (Figures 9A and 9B). The mice also had a significant reduction in both
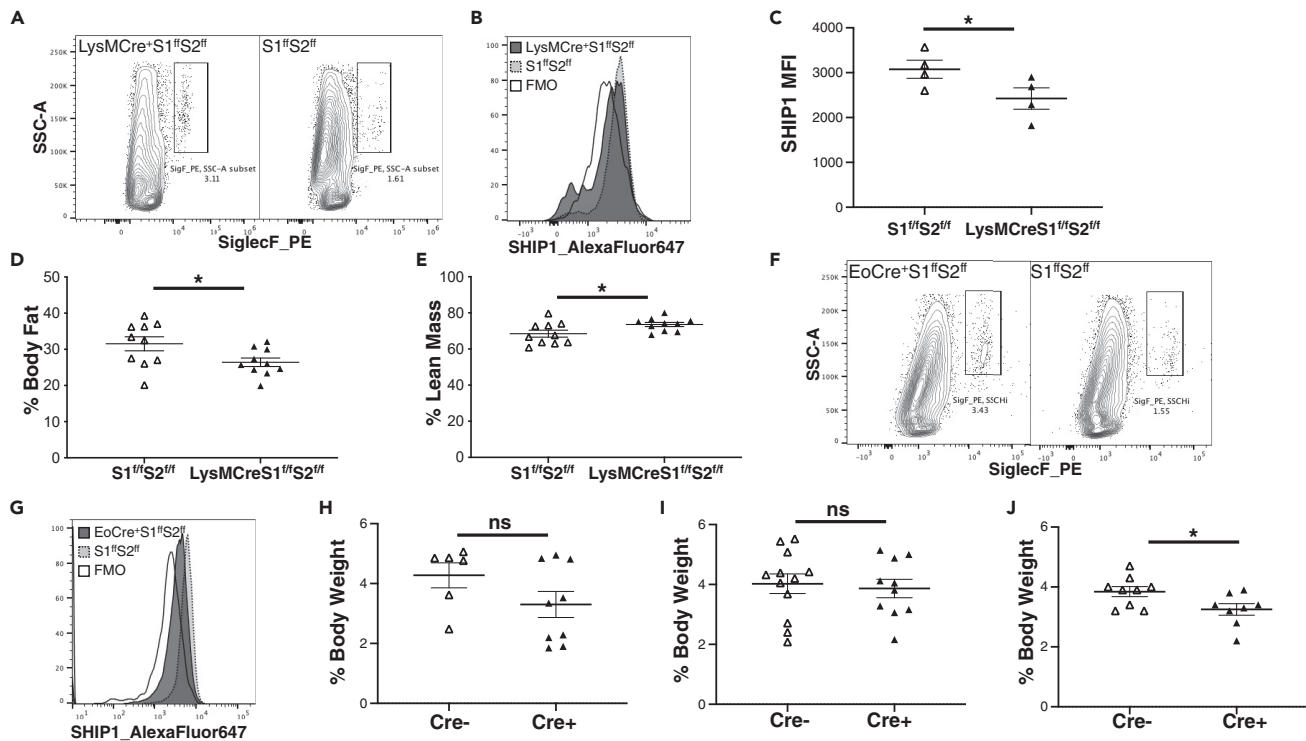
Figure 8. Genetic ablation of both SHIP paralogs in eosinophils and/or myeloid cells limits diet-induced increases in adiposity

(A) Representative gating for total eosinophils (Live, CD45$^+$, SSC^{HI}SigF$^+$) and (B) histograms of SHIP1 staining from eosinophils (in A) in the eWAT of a LysMCreSHIP1$^{flox/flox}$SHIP2$^{flox/flox}$ mouse or a SHIP1$^{flox/flox}$SHIP2$^{flox/flox}$ littermate. FMO control stain was performed with a mix of eWAT leukocytes from both genotypes.

(C) MFI of SHIP1 in eosinophils from LysMCreSHIP1$^{flox/flox}$SHIP2$^{flox/flox}$ and SHIP1$^{flox/flox}$SHIP2$^{flox/flox}$ littermate controls.

(D) Percent body fat and (E) percent lean mass as determined by DEXA analysis in LysMCreSHIP1$^{flox/flox}$SHIP2$^{flox/flox}$ and their SHIP1$^{flox/flox}$SHIP2$^{flox/flox}$ littermates after 8 weeks on HFD.

(F) Representative gating for eosinophils (Live, CD45$^+$, SSC^{HI}SigF$^+$) (G) histograms of SHIP1 staining in eosinophils (F) in the eWAT of an eoCreSHIP1$^{flox/flox}$SHIP2$^{flox/flox}$ mouse or a SHIP1$^{flox/flox}$SHIP2$^{flox/flox}$ littermate. FMO control stain was performed with a mix of eWAT leukocytes from both genotypes. Percentage of total body weight for the iWAT fat pad in (H) eoCreSHIP1$^{flox/flox}$, (I) eoCreSHIP2$^{flox/flox}$ and (J) eoCreSHIP1$^{flox/flox}$SHIP2$^{flox/flox}$ cohorts versus their corresponding SHIP$^{flox/flox}$ littermate controls after 12 weeks on HFD, unpaired two-tailed t-test, *p < 0.05; ns, p > 0.05).

iWAT and eWAT fat pad mass after the 4-week treatment with K161 (Figure 9C). In addition, blood glucose levels in the K161-treated cohort were also lower than in the vehicle treated cohort (Figure 9D). We then measured serum IL5 and found that the K161 treated mice had a significantly higher amount of IL5 as compared to vehicle controls (Figure 9E). This suggested that the ILC2 function might also be promoted by K161 treatment. Although we do not observe a significant increase in the frequency or number of ILC2 in the VAT of aged mice with K161 treatment (Figures 9F–9H and S6), we do find that their surface expression of the IL133R (ST2) is increased by K161 treatment (Figure 9I). Various cell signaling modulators have previously been shown to alter ST2 levels on T cells and ILC2.[57,58] Importantly, we find that K161 treatment significantly increases the frequency of the IL13 producing subset of ILC2 as well as their production of IL13 on a per cell basis (Figures 9J-9M). Thus, pan-SHIPi also has the capacity to promote an ILC2 function, IL13 production. This might potentially be related to increased IL33R signaling because IL33R surface expression is up-regulated by K161 on ILC2 and IL33 has been shown to induce IL13 expression by Treg cells.[59] This activity of K161 on the ILC2 compartment could potentially contribute to control of obesity in the setting of aging.

Pan-SHIP1/2 inhibitors mediate control of blood sugar levels independent of their effect on adiposity and eosinophils

In our previous study we found that K118 also improves blood glucose regulation in obese mice.[42] We found this also to be the case with the pan-SHIP1/2 inhibitors K149 (Figure 10A) and K161 (Figure 10C) as they both reduced blood glucose levels in mice after 6 weeks of HFD consumption as compared to
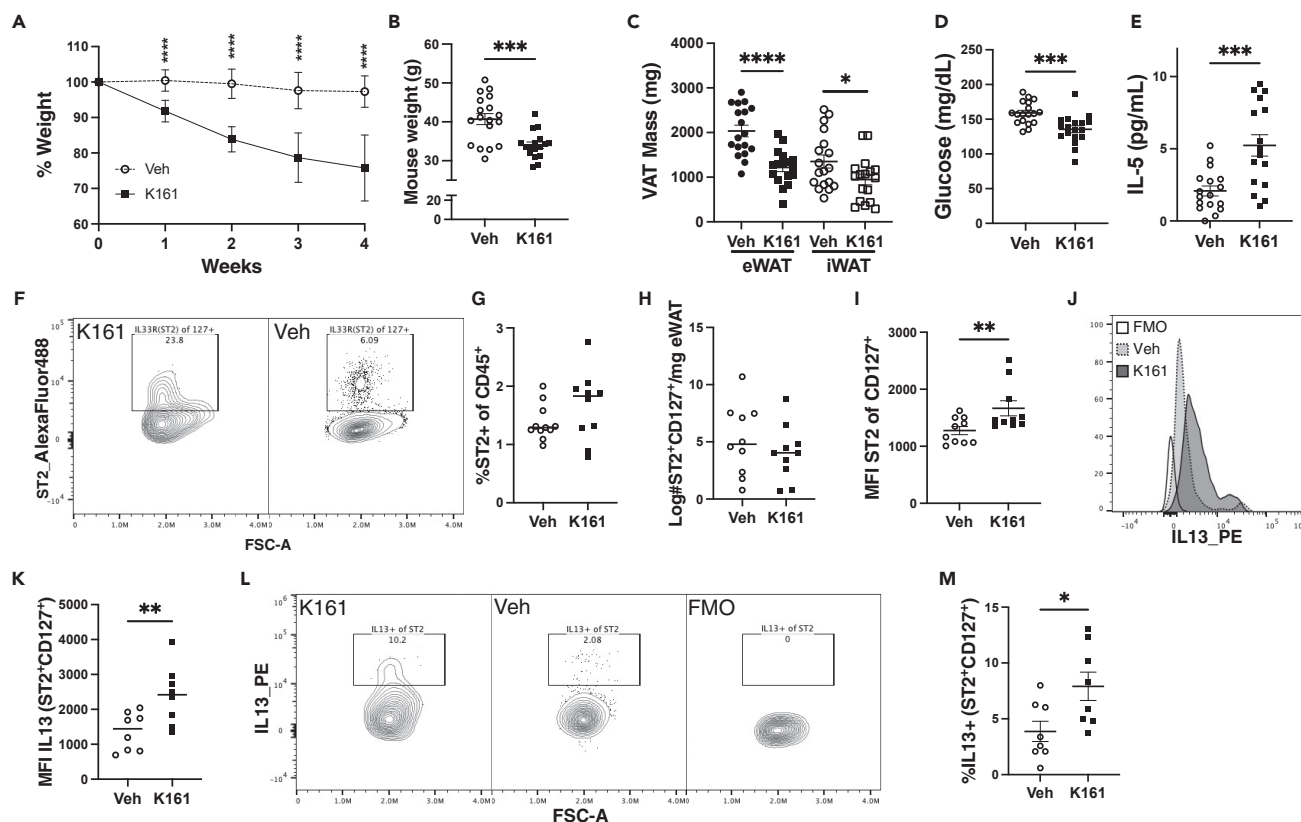
Figure 9. The pan-SHIP1/2 inhibitor K161 reduces adiposity and increases ILC2 frequency and function in obesity associated with aging

Aged mice (10 months old) that only consumed normal chow but had become obese (>32g body mass at study initiation) were treated twice a week for 4 weeks with K161 as described previously.

(A) Percent weight change after initiation of K161 or vehicle treatment for 4 weeks. Endpoint mouse weight (g) (B) eWAT and iWAT fat pads weights (C) after 4 weeks of K161 or vehicle treatment.

(D) *Ad libitum* blood glucose measurements 3 weeks after initiation of K161 or vehicle treatment.

(E) Endpoint (4 weeks) serum IL5 levels of K161 or vehicle treated mice.

(F) Representative final gating for ILC2 (Live, Lin$^-$CD45$^+$Sca1$^+$CD117(c-Kit)$^-$CD127(IL7Rα)$^+$ST2(IL33R)$^+$ (See Figure S6 for gating strategy) (G) ST2 (IL33R)$^+$ cell frequency of CD45$^+$, and (H) absolute number per gram of eWAT. (I) MFI of ST2 (IL33R) in Live, Lin$^-$CD45$^+$Sca1$^+$CD117(c-Kit)$^-$CD127(IL7Rα)$^+$ cells. Representative expression (J) and MFI (K) of IL13 and representative flow plots (L) and frequency of IL13 cells (M) within the ILC2 cell compartment present in eWAT of K161 or vehicle treated mice. (*$p < 0.05$, **$p < 0.01$, ***$p < 0.001$, ****$p < 0.0001$, Unpaired one-tailed t-test with Welch's correction when needed).

vehicle controls. We also tested this in the setting of obesity treatment with K161, where mice become obese following 2 months of HFD consumption and then were treated for two weeks with K161 or vehicle while continuing to consume HFD. We found that K161 also mediated a significant reduction in blood glucose levels versus vehicle controls (Figure 10E). We speculated this might have simply been a byproduct of obesity control. However, this appears to be an entirely independent effect of pan-SHIP1/2 inhibition as K149 (Figure 10B) or K161 (Figure 10D) treated ΔdblGATA mice still show significant reductions in blood glucose versus vehicle controls in an obesity prevention setting, despite the fact that percent body fat is not decreased in ΔdblGATA versus vehicle controls treated with either K149 or K161 (Figure 7). We also found that K161 significantly reduced blood glucose levels in obese ΔdblGATA mice (Figure 10F). Thus, pan-SHIP1/2 inhibitors can improve blood glucose control in the setting of increased caloric intake and frank obesity, and do so independent of their ability to reduce adiposity via the eosinophil compartment.

DISCUSSION

Here we show that SHIP inhibitory compounds capable of inhibiting both SHIP1 and SHIP2 are optimal for reducing obesity associated with excess caloric intake. We show that this is the case for both aminosteroid- and tryptamine-based pan-SHIP1/2 inhibitors. However, compounds that only selectively inhibit SHIP1 or SHIP2 are completely ineffective at preventing accumulation of excess body fat associated with excess
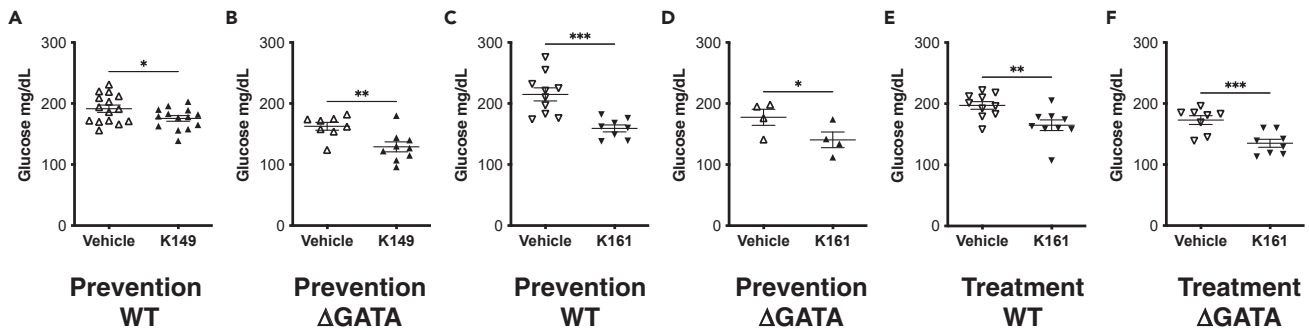
Figure 10. Pan-SHIP1/2 inhibitors mediate control of blood sugar levels independent of their effect on adiposity and eosinophils
Endpoint *ad libitum* blood glucose levels were measured in (A, C, E) C57BL/6 or (B, D, F) ΔdblGATA mice following treatment with pan-SHIP1/2 inhibitors (A, B) K149 or vehicle (5% DMSO:saline) or (C–F) K161 or vehicle (H$_2$O). Measurements were performed 16h after the final dose of SHIPi from mice treated above. SHIPi was initiated on the same day that mice were place on HFD for the prevention model (A-D) whereas mice were placed on HFD for 8 weeks before initiation and maintained for the duration SHIPi in treatment model (E, F) (*p < 0.05, **p < 0.01, ***p < 0.001, ****p < 0.0001, Unpaired one-tailed t-test with Welch's correction when needed).

caloric intake and yet when these same two paralog-selective inhibitors are co-administered to mice consuming a HFD the combination protects from increased accumulation of body fat. We find that the eosinophil compartment is required for promotion of the lean state by pan-SHIP1/2 inhibitors. This activity is correlated with the ability of pan-SHIP1/2 inhibitors to increase the frequency and function of VAT-resident ILC2 producing IL13, the frequency of IL4-producing eosinophils in VAT and polarization of the VAT macrophage compartment toward M2 macrophages. Consistent with these pharmacological approaches, conditional knockout of both SHIP paralogs in myeloid cells and/or eosinophils also reduces adiposity - in particular SHIP paralog ablation limits accumulation of abdominal fat mass. Surprisingly, the ability of pan-SHIP1/2 inhibitors to improve blood glucose control is not linked to their capacity to prevent increased body fat accumulation, indicating their ability to improve glucose control has a distinct mechanism of action.

Control of both obesity and blood glucose levels by immune cells present in the VAT is now understood to have a prominent role in metabolic control, and also its dysregulation.[1–3,7–18,20] The recently described M1-like inflammatory macrophage subsets in VAT that can act as norepinephrine (NE) sinks may have provided the much sought after 'missing-link' between VAT immune function and energy utilization by lipid-laden adipocytes.[4–6] However, direct production of NE by M2 macrophages to stimulate lipolysis and thermogenesis by VAT adipocytes remains a distinct possibility.[16,20] In fact, there is likely a competition between these distinct macrophage functions that ultimately tips the balance toward metabolic control or dysregulation during sustained intake of excess calories. Of the cells present in the VAT immune milieu, we find that pan-SHIP1/2 inhibition requires an eosinophil compartment to mediate obesity control. How pan-SHIP1/2 inhibitors achieve this effect on adiposity via eosinophils remains to be defined. However, pan-SHIP1/2 inhibition was consistently found to increase the frequency of IL4-producing eosinophils in the VAT as well as the amount of IL4 they produce on a per cell basis. IL4 production by VAT eosinophils can drive polarization of the local myeloid compartment in VAT toward cells of an M2 phenotype[15] and M2 polarization was consistently observed with all three pan-SHIP1/2 inhibitors tested in HFD obesity models used here. Whether this also leads to catecholamine synthesis by M2 cells remains to be determined. Another possibility, however, is that M2 polarization reduces the inflammatory M1 macrophages in VAT that can sequester NE from adipocytes and thereby increases β-adrenergic signaling in the adipocyte compartment indirectly. One or both are possibilities that might be explored to better understand how pan-SHIP1/2 inhibition mediates obesity control via the eosinophil compartment and their influence on macrophage differentiation in the VAT.

Analysis of K161 treatment in aged mice that had become obese even while consuming a normal caloric diet is the first demonstration of a significant positive effect of pan-SHIPi on the function of the ILC2 compartment – the apex cell of the immune circuit that regulates energy consumption and storage in the VAT.[18,52,60] This was somewhat surprising as we had not observed a significant increase in VAT ILC2 function with K118 treatment in young adult mice consuming an HFD.[42] The reason for this difference could be the strength of the adipogenic stressor (HFD versus normal chow in aging) or may simply reflect the fact

that K161 is a more potent inhibitor that has better bioavailability *in vivo* due to its water solubility.[40,41] Nonetheless, our findings with K161 indicate it is possible for pan-SHIPi to act at all the major stages of this immune cell circuit in VAT, including ILC2. Our genetic findings indicate that dual paralog inactivation may in fact render eosinophils or M2 cells that are downstream of ILC2 more responsive to the cytokines and other factors they produce as part of their homeostatic function in VAT (e.g., IL5, IL13). The responsiveness of double SHIP KO eosinophils (versus single paralog SHIP KO) to factors elaborated by ILC2 might now be investigated to determine whether enhanced ILC2 function in the VAT can in fact further amplify the effects that pan-SHIPi compounds directly exert on these more distal immune cells in obesity control – as suggested by our conditional knockout studies of both paralogs in eosinophils and the myeloid compartment.

We had previously shown that K118 improves blood glucose control, including the ability of the host to sequester glucose from the plasma.[42] We found that the more potent and water-soluble aminosteroid pan-SHIP1/2 inhibitor K161 and the tryptamine K149 also improved blood glucose control in both HFD obesity models. However, it was surprising to find pan-SHIP1/2 inhibitors mediate blood glucose control in ΔdblGATA mutant mice that lack eosinophils which are resistant to obesity control by pan-SHIP1/2 inhibitors. This indicates a separate and distinct mechanism of action for blood glucose control by pan-SHIP1/2 inhibitors that does not require eosinophil function and their polarization of the macrophage compartment toward an M2 phenotype. Toward that end, it is possible that blood glucose control by pan-SHIP1/2 inhibitors could be acting via the VAT Treg compartment. The VAT Treg compartment exerts profound control over blood glucose levels in obesity.[8,14] In our previous study, we found that the pan-SHIP1/2 inhibitor K118 prevents the progressive diminution of tissue-resident Treg cells in the VAT during obesity.[42] Thus, it is possible that these compounds can act to prevent the demise of tissue-resident Treg compartment in the VAT of obese mice to maintain or improve blood glucose regulation. Consistent with this hypothesis, genetic SHIP1 deficiency increases the number and function of Treg cells in the spleen and lymph nodes through both cell-intrinsic and-extrinsic pathways.[29,61] Alternatively, this could be due to the SHIP2 inhibitory effect of the pan-SHIP1/2 inhibitors, as the SHIP2 selective inhibitor AS1949490 improves glucose control in diabetic *db/db* mice[31] and SHIP2$^{-/-}$ mutant mice maintain normal glucose control when placed on an HFD.[30]

Obesity, and the metabolic dysregulation that accompanies it, are major emerging challenges for global health. Thus, novel treatments are needed to combat obesity and its diabetic consequences. We have shown here that multiple SHIP1/2 inhibitors of two different chemical classes not only combat body fat accumulation associated with excess caloric intake, but also improve the control of plasma glucose levels. Intriguingly, they appear to act primarily by promoting homeostatic function of innate immune cells found in VAT, although their impact on glucose control may be due to effects on non-immune cells that express only the SHIP2 paralog. Further research is thus needed to increase our understanding of how these compounds achieve both of these metabolic effects. Nonetheless, pan-SHIP1/2 inhibitory small molecules represent promising candidates for drug development in both obesity and diet-induced diabetes. Further, this study illustrates the potential of targeting innate immune components present in VAT for control of obesity caused by dietary practices and aging.

Limitations of the study

As with any study utilizing small molecules that impact the function of key signaling molecules, like SHIP1 and SHIP2, one or all of the molecules we utilize here could potentially have 'off-target' effects that also impact host physiology. However, it is high unlikely that unknown off-target effects of these molecules are responsible for their control of obesity since (1) the pan-SHIPi compounds described here are of distinct chemical classes, (2) dual treatment with the SHIP1-selective inhibitor 3AC and the SHIP2-selective inhibitor AS1949490 also mediated control of obesity and (3) genetic inactivation of both SHIP1 and SHIP2, but not either paralog alone, reduced diet-induced obesity. We show that conditional knockout of SHIP1 and SHIP2 in all myeloid cells or eosinophils was sufficient to mediate reduced diet-induced obesity with the largest effect seen with the pan-myeloid LysMCre driver of gene ablation. It will be important to further refine this genetic analysis with Cre drivers that have more restricted expression of Cre recombinase in distinct macrophage populations, for example the CxCX3CR1-Cre^{ERT2} driver or perhaps Cre drivers that delete selectively in M1 or M2 macrophages. Although we show that M2 polarization if induced by all pan-SHIPi compounds it is important that eventually a more comprehensive analysis all macrophage subtypes in pan-SHIPi treated hosts is conducted, including inflammatory macrophage subsets that have

recently been identified in close proximity with peripheral nerves in visceral fat and that act as sinks for norepinephrine to limit thermogenesis in DIO and aging. Pan-SHIPi mediated reduced hyperglycemia in mice that lack eosinophils, thus it will be interesting to explore the impact of dual gene inactivation of SHIP1 and SHIP2 in Treg cells and other cell types given the precise role that these immunoregulatory T cells play in control of glucose levels.

STAR★METHODS

Detailed methods are provided in the online version of this paper and include the following:

- KEY RESOURCES TABLE
- RESOURCE AVAILABILITY
  - Lead contact
  - Materials availability
  - Data and code availability
- EXPERIMENTAL MODEL AND SUBJECT DETAILS
  - Mice
  - SHIP inhibitor treatment of mice
  - Detection of immune cells in adipose tissue by flow cytometry
  - Treatment of C2 cells with SHIP inhibitors
  - Blood glucose
  - IL5 ELISA
  - DEXA analysis
- QUANTIFICATION AND STATISTICAL ANALYSIS

SUPPLEMENTAL INFORMATION

Supplemental information can be found online at https://doi.org/10.1016/j.isci.2023.106071.

ACKNOWLEDGMENTS

AUTHOR CONTRIBUTIONS

DECLARATION OF INTERESTS

W.G.K, S.F., C.P. and J.D.C have patents, pending and issued, concerning the analysis and targeting of SHIP1 and SHIP2 in disease. The other authors have no interests to declare.

REFERENCES

1. Weisberg, S.P., McCann, D., Desai, M., Rosenbaum, M., Leibel, R.L., and Ferrante, A.W., Jr. (2003). Obesity is associated with macrophage accumulation in adipose tissue. J. Clin. Invest. 112, 1796–1808. https://doi.org/10.1172/JCI19246.

2. Weisberg, S.P., Hunter, D., Huber, R., Lemieux, J., Slaymaker, S., Vaddi, K., Charo, I., Leibel, R.L., and Ferrante, A.W., Jr. (2006). CCR2 modulates inflammatory and metabolic effects of high-fat feeding. J. Clin. Invest. 116, 115–124. https://doi.org/10.1172/JCI24335.

3. Xu, H., Barnes, G.T., Yang, Q., Tan, G., Yang, D., Chou, C.J., Sole, J., Nichols, A., Ross, J.S., Tartaglia, L.A., and Chen, H. (2003). Chronic inflammation in fat plays a crucial role in the development of obesity-related insulin resistance. J. Clin. Invest. 112, 1821–1830. https://doi.org/10.1172/JCI19451.

4. Pirzgalska, R.M., Seixas, E., Seidman, J.S., Link, V.M., Sánchez, N.M., Mahú, I., Mendes, R., Gres, V., Kubasova, N., Morris, I., et al. (2017). Sympathetic neuron-associated macrophages contribute to obesity by importing and

metabolizing norepinephrine. Nat. Med. *23*, 1309–1318. https://doi.org/10.1038/nm.4422.

5. Camell, C.D., Sander, J., Spadaro, O., Lee, A., Nguyen, K.Y., Wing, A., Goldberg, E.L., Youm, Y.H., Brown, C.W., Elsworth, J., et al. (2017). Inflammasome-driven catecholamine catabolism in macrophages blunts lipolysis during ageing. Nature *550*, 119–123. https://doi.org/10.1038/nature24022.

6. Pirzgalska, R.M., and Domingos, A.I. (2018). Macrophages in obesity. Cell. Immunol. *330*, 183–187. https://doi.org/10.1016/j.cellimm.2018.04.014.

7. Chawla, A., Nguyen, K.D., and Goh, Y.P.S. (2011). Macrophage-mediated inflammation in metabolic disease. Nat. Rev. Immunol. *11*, 738–749. https://doi.org/10.1038/nri3071.

8. Feuerer, M., Herrero, L., Cipolletta, D., Naaz, A., Wong, J., Nayer, A., Lee, J., Goldfine, A.B., Benoist, C., Shoelson, S., and Mathis, D. (2009). Lean, but not obese, fat is enriched for a unique population of regulatory T cells that affect metabolic parameters. Nat. Med. *15*, 930–939. https://doi.org/10.1038/nm.2002.

9. Lumeng, C.N., Bodzin, J.L., and Saltiel, A.R. (2007). Obesity induces a phenotypic switch in adipose tissue macrophage polarization. J. Clin. Invest. *117*, 175–184. https://doi.org/10.1172/JCI29881.

10. Odegaard, J.I., and Chawla, A. (2011). Alternative macrophage activation and metabolism. Annu. Rev. Pathol. *6*, 275–297. https://doi.org/10.1146/annurev-pathol-011110-130138.

11. Ostrand-Rosenberg, S. (2018). Myeloid derived-suppressor cells: their role in cancer and obesity. Curr. Opin. Immunol. *51*, 68–75. https://doi.org/10.1016/j.coi.2018.03.007.

12. Xia, S., Sha, H., Yang, L., Ji, Y., Ostrand-Rosenberg, S., and Qi, L. (2011). Gr-1+ CD11b+ myeloid-derived suppressor cells suppress inflammation and promote insulin sensitivity in obesity. J. Biol. Chem. *286*, 23591–23599. https://doi.org/10.1074/jbc.M111.237123.

13. Kolodin, D., van Panhuys, N., Li, C., Magnuson, A.M., Cipolletta, D., Miller, C.M., Wagers, A., Germain, R.N., Benoist, C., and Mathis, D. (2015). Antigen- and cytokine-driven accumulation of regulatory T cells in visceral adipose tissue of lean mice. Cell Metab. *21*, 543–557. https://doi.org/10.1016/j.cmet.2015.03.005.

14. Li, C., Spallanzani, R.G., and Mathis, D. (2020). Visceral adipose tissue Tregs and the cells that nurture them. Immunol. Rev. *295*, 114–125. https://doi.org/10.1111/imr.12850.

15. Wu, D., Molofsky, A.B., Liang, H.E., Ricardo-Gonzalez, R.R., Jouihan, H.A., Bando, J.K., Chawla, A., and Locksley, R.M. (2011). Eosinophils sustain adipose alternatively activated macrophages associated with glucose homeostasis. Science *332*, 243–247. https://doi.org/10.1126/science.1201475.

16. Nguyen, K.D., Qiu, Y., Cui, X., Goh, Y.P.S., Mwangi, J., David, T., Mukundan, L., Brombacher, F., Locksley, R.M., and Chawla,

A. (2011). Alternatively activated macrophages produce catecholamines to sustain adaptive thermogenesis. Nature *480*, 104–108. https://doi.org/10.1038/nature10653.

17. Molofsky, A.B., Nussbaum, J.C., Liang, H.E., Van Dyken, S.J., Cheng, L.E., Mohapatra, A., Chawla, A., and Locksley, R.M. (2013). Innate lymphoid type 2 cells sustain visceral adipose tissue eosinophils and alternatively activated macrophages. J. Exp. Med. *210*, 535–549. https://doi.org/10.1084/jem.20121964.

18. Brestoff, J.R., Kim, B.S., Saenz, S.A., Stine, R.R., Monticelli, L.A., Sonnenberg, G.F., Thome, J.J., Farber, D.L., Lutfy, K., Seale, P., and Artis, D. (2015). Group 2 innate lymphoid cells promote beiging of white adipose tissue and limit obesity. Nature *519*, 242–246. https://doi.org/10.1038/nature14115.

19. Fischer, K., Ruiz, H.H., Jhun, K., Finan, B., Oberlin, D.J., van der Heide, V., Kalinovich, A.V., Petrovic, N., Wolf, Y., Clemmensen, C., et al. (2017). Alternatively activated macrophages do not synthesize catecholamines or contribute to adipose tissue adaptive thermogenesis. Nat. Med. *23*, 623–630. https://doi.org/10.1038/nm.4316.

20. Zhao, H., Shang, Q., Pan, Z., Bai, Y., Li, Z., Zhang, H., Zhang, Q., Guo, C., Zhang, L., and Wang, Q. (2018). Exosomes from adipose-derived stem cells attenuate adipose inflammation and obesity through polarizing M2 macrophages and beiging in white adipose tissue. Diabetes *67*, 235–247. https://doi.org/10.2337/db17-0356.

21. Helgason, C.D., Damen, J.E., Rosten, P., Grewal, R., Sorensen, P., Chappel, S.M., Borowski, A., Jirik, F., Krystal, G., and Humphries, R.K. (1998). Targeted disruption of SHIP leads to hemopoietic perturbations, lung pathology, and a shortened life span. Genes Dev. *12*, 1610–1620.

22. Desponts, C., Hazen, A.L., Paraiso, K.H.T., and Kerr, W.G. (2006). SHIP deficiency enhances HSC proliferation and survival but compromises homing and repopulation. Blood *107*, 4338–4345. https://doi.org/10.1182/blood-2005-12-5021.

23. Helgason, C.D., Antonchuk, J., Bodner, C., and Humphries, R.K. (2003). Homeostasis and regeneration of the hematopoietic stem cell pool are altered in SHIP-deficient mice. Blood *102*, 3541–3547.

24. Brauweiler, A., Tamir, I., Dal Porto, J., Benschop, R.J., Helgason, C.D., Humphries, R.K., Freed, J.H., and Cambier, J.C. (2000). Differential regulation of B cell development, activation, and death by the src homology 2 domain-containing 5' inositol phosphatase (SHIP). J. Exp. Med. *191*, 1545–1554.

25. Helgason, C.D., Kalberer, C.P., Damen, J.E., Chappel, S.M., Pineault, N., Krystal, G., and Humphries, R.K. (2000). A dual role for Src homology 2 domain-containing inositol-5-phosphatase (SHIP) in immunity: aberrant development and enhanced function of b lymphocytes in ship -/- mice. J. Exp. Med. *191*, 781–794.

26. Sly, L.M., Rauh, M.J., Kalesnikoff, J., Song, C.H., and Krystal, G. (2004). LPS-induced upregulation of SHIP is essential for endotoxin tolerance. Immunity *21*, 227–239.

27. Wang, J.W., Howson, J.M., Ghansah, T., Desponts, C., Ninos, J.M., May, S.L., Nguyen, K.H.T., Toyama-Sorimachi, N., and Kerr, W.G. (2002). Influence of SHIP on the NK repertoire and allogeneic bone marrow transplantation. Science *295*, 2094–2097.

28. Park, M.Y., Srivastava, N., Sudan, R., Viernes, D.R., Chisholm, J.D., Engelman, R.W., and Kerr, W.G. (2014). Impaired T-cell survival promotes mucosal inflammatory disease in SHIP1-deficient mice. Mucosal Immunol. *7*, 1429–1439. https://doi.org/10.1038/mi.2014.32.

29. Collazo, M.M., Wood, D., Paraiso, K.H.T., Lund, E., Engelman, R.W., Le, C.T., Stauch, D., Kotsch, K., and Kerr, W.G. (2009). SHIP limits immunoregulatory capacity in the T-cell compartment. Blood *113*, 2934–2944. https://doi.org/10.1182/blood-2008-09-181164.

30. Sleeman, M.W., Wortley, K.E., Lai, K.M.V., Gowen, L.C., Kintner, J., Kline, W.O., Garcia, K., Stitt, T.N., Yancopoulos, G.D., Wiegand, S.J., and Glass, D.J. (2005). Absence of the lipid phosphatase SHIP2 confers resistance to dietary obesity. Nat. Med. *11*, 199–205. https://doi.org/10.1038/nm1178.

31. Suwa, A., Yamamoto, T., Sawada, A., Minoura, K., Hosogai, N., Tahara, A., Kurama, T., Shimokawa, T., and Aramori, I. (2009). Discovery and functional characterization of a novel small molecule inhibitor of the intracellular phosphatase, SHIP2. Br. J. Pharmacol. *158*, 879–887. https://doi.org/10.1111/j.1476-5381.2009.00358.x.

32. Kam, T.I., Park, H., Gwon, Y., Song, S., Kim, S.H., Moon, S.W., Jo, D.G., and Jung, Y.K. (2016). FcgammaRIIb-SHIP2 axis links Abeta to tau pathology by disrupting phosphoinositide metabolism in Alzheimer's disease model. Elife *5*, e18691. https://doi.org/10.7554/eLife.18691.

33. Fuhler, G.M., Brooks, R., Toms, B., Iyer, S., Gengo, E.A., Park, M.Y., Gumbleton, M., Viernes, D.R., Chisholm, J.D., and Kerr, W.G. (2012). Therapeutic potential of SH2 domain-containing inositol-5'-phosphatase 1 (SHIP1) and SHIP2 inhibition in cancer. Mol. Med. *18*, 65–75. https://doi.org/10.2119/molmed.2011.00178.

34. Chen, Z., Shojaee, S., Buchner, M., Geng, H., Lee, J.W., Klemm, L., Titz, B., Graeber, T.G., Park, E., Tan, Y.X., et al. (2015). Signalling thresholds and negative B-cell selection in acute lymphoblastic leukaemia. Nature *521*, 357–361. https://doi.org/10.1038/nature14231.

35. Fernandes, S., Brooks, R., Gumbleton, M., Park, M.Y., Russo, C.M., Howard, K.T., Chisholm, J.D., and Kerr, W.G. (2015). SHIPi enhances autologous and allogeneic hematolymphoid stem cell transplantation. EBioMedicine *2*, 205–213. https://doi.org/10.1016/j.ebiom.2015.02.004.

36. Brooks, R., Fuhler, G.M., Iyer, S., Smith, M.J., Park, M.Y., Paraiso, K.H.T., Engelman, R.W.,

and Kerr, W.G. (2010). SHIP1 inhibition increases immunoregulatory capacity and triggers apoptosis of hematopoietic cancer cells. J. Immunol. *184*, 3582–3589. https://doi.org/10.4049/jimmunol.0902844.

37. Brooks, R., Iyer, S., Akada, H., Neelam, S., Russo, C.M., Chisholm, J.D., and Kerr, W.G. (2015). Coordinate expansion of murine hematopoietic and mesenchymal stem cell compartments by SHIPi. Stem Cell. *33*, 848–858. https://doi.org/10.1002/stem.1902.

38. Gumbleton, M., Sudan, R., Fernandes, S., Engelman, R.W., Russo, C.M., Chisholm, J.D., and Kerr, W.G. (2017). Dual enhancement of T and NK cell function by pulsatile inhibition of SHIP1 improves antitumor immunity and survival. Sci. Signal. *10*, eaam5353. https://doi.org/10.1126/scisignal.aam5353.

39. Saz-Leal, P., Del Fresno, C., Brandi, P., Martínez-Cano, S., Dungan, O.M., Chisholm, J.D., Kerr, W.G., and Sancho, D. (2018). Targeting SHIP-1 in myeloid cells enhances trained immunity and boosts response to infection. Cell Rep. *25*, 1118–1126. https://doi.org/10.1016/j.celrep.2018.09.092.

40. Pedicone, C., Fernandes, S., Dungan, O.M., Dormann, S.M., Viernes, D.R., Adhikari, A.A., Choi, L.B., De Jong, E.P., Chisholm, J.D., and Kerr, W.G. (2020). Pan-SHIP1/2 inhibitors promote microglia effector functions essential for CNS homeostasis. J. Cell Sci. *133*, jcs238030. https://doi.org/10.1242/jcs.238030.

41. Kerr, W.G., Pedicone, C., Dormann, S., Pacherille, A., and Chisholm, J.D. (2020). Small molecule targeting of SHIP1 and SHIP2. Biochem. Soc. Trans. *48*, 291–300. https://doi.org/10.1042/BST20190775.

42. Srivastava, N., Iyer, S., Sudan, R., Youngs, C., Engelman, R.W., Howard, K.T., Russo, C.M., Chisholm, J.D., and Kerr, W.G. (2016). A small-molecule inhibitor of SHIP1 reverses age- and diet-associated obesity and metabolic syndrome. JCI Insight *1*, e88544. https://doi.org/10.1172/jci.insight.88544.

43. Itkin, T., Kumari, A., Schneider, E., Gur-Cohen, S., Ludwig, C., Brooks, R., Kollet, O., Golan, K., Khatib-Massalha, E., Russo, C.M., et al. (2017). MicroRNA-155 promotes G-CSF-induced mobilization of murine hematopoietic stem and progenitor cells via propagation of CXCL12 signaling. Leukemia *31*, 1247–1250. https://doi.org/10.1038/leu.2017.50.

44. Ichihara, Y., Fujimura, R., Tsuneki, H., Wada, T., Okamoto, K., Gouda, H., Hirono, S., Sugimoto, K., Matsuya, Y., Sasaoka, T., and Toyooka, N. (2013). Rational design and synthesis of 4-substituted 2-pyridin-2-ylamides with inhibitory effects on SH2 domain-containing inositol 5′-phosphatase 2 (SHIP2). Eur. J. Med. Chem. *62*, 649–660. https://doi.org/10.1016/j.ejmech.2013.01.014.

45. Hoekstra, E., Das, A.M., Willemsen, M., Swets, M., Kuppen, P.J.K., van der Woude, C.J., Bruno, M.J., Shah, J.P., Ten Hagen, T.L.M., Chisholm, J.D., et al. (2016). Lipid phosphatase SHIP2 functions as oncogene in colorectal cancer by regulating PKB activation. Oncotarget *7*, 73525–73540. https://doi.org/10.18632/oncotarget.12321.

46. Fernandes, S., Meyer, S.T., Shah, J.P., Adhikari, A.A., Kerr, W.G., and Chisholm, J.D. (2022). N1-Benzyl tryptamine pan-SHIP1/2 inhibitors: synthesis and preliminary biological evaluation as anti-tumor agents. Molecules *27*, 8451. https://doi.org/10.3390/molecules27238451.

47. Scheid, M.P., Huber, M., Damen, J.E., Hughes, M., Kang, V., Neilsen, P., Prestwich, G.D., Krystal, G., and Duronio, V. (2002). Phosphatidylinositol (3,4,5)P3 is essential but not sufficient for protein kinase B (PKB) activation; phosphatidylinositol (3,4)P2 is required for PKB phosphorylation at Ser-473: studies using cells from SH2-containing inositol-5-phosphatase knockout mice. J. Biol. Chem. *277*, 9027–9035. https://doi.org/10.1074/jbc.M106755200.

48. Franke, T.F., Kaplan, D.R., Cantley, L.C., and Toker, A. (1997). Direct regulation of the Akt proto-oncogene product by phosphatidylinositol-3,4-bisphosphate. Science *275*, 665–668. https://doi.org/10.1126/science.275.5300.665.

49. Gozzelino, L., De Santis, M.C., Gulluni, F., Hirsch, E., and Martini, M. (2020). PI(3,4)P2 signaling in cancer and metabolism. Front. Oncol. *10*, 360. https://doi.org/10.3389/fonc.2020.00360.

50. Qiu, Y., Nguyen, K.D., Odegaard, J.I., Cui, X., Tian, X., Locksley, R.M., Palmiter, R.D., and Chawla, A. (2014). Eosinophils and type 2 cytokine signaling in macrophages orchestrate development of functional beige fat. Cell *157*, 1292–1308. https://doi.org/10.1016/j.cell.2014.03.066.

51. Yu, C., Cantor, A.B., Yang, H., Browne, C., Wells, R.A., Fujiwara, Y., and Orkin, S.H. (2002). Targeted deletion of a high-affinity GATA-binding site in the GATA-1 promoter leads to selective loss of the eosinophil lineage in vivo. J. Exp. Med. *195*, 1387–1395.

52. Nussbaum, J.C., Van Dyken, S.J., von Moltke, J., Cheng, L.E., Mohapatra, A., Molofsky, A.B., Thornton, E.E., Krummel, M.F., Chawla, A., Liang, H.E., and Locksley, R.M. (2013). Type 2 innate lymphoid cells control eosinophil homeostasis. Nature *502*, 245–248. https://doi.org/10.1038/nature12526.

53. Clausen, B.E., Burkhardt, C., Reith, W., Renkawitz, R., and Förster, I. (1999). Conditional gene targeting in macrophages and granulocytes using LysMcre mice. Transgenic Res. *8*, 265–277.

54. Abram, C.L., Roberge, G.L., Hu, Y., and Lowell, C.A. (2014). Comparative analysis of the efficiency and specificity of myeloid-Cre deleting strains using ROSA-EYFP reporter mice. J. Immunol. Methods *408*, 89–100. https://doi.org/10.1016/j.jim.2014.05.009.

55. Zhu, C., Xia, L., Li, F., Zhou, L., Weng, Q., Li, Z., Wu, Y., Mao, Y., Zhang, C., Wu, Y., et al. (2018). mTOR complexes differentially orchestrates eosinophil development in allergy. Sci. Rep. *8*, 6883. https://doi.org/10.1038/s41598-018-25358-z.

56. Doyle, A.D., Jacobsen, E.A., Ochkur, S.I., Willetts, L., Shim, K., Neely, J., Kloeber, J., Lesuer, W.E., Pero, R.S., Lacy, P., et al. (2013). Homologous recombination into the eosinophil peroxidase locus generates a strain of mice expressing Cre recombinase exclusively in eosinophils. J. Leukoc. Biol. *94*, 17–24. https://doi.org/10.1189/jlb.0213089.

57. Chen, T., Tibbitt, C.A., Feng, X., Stark, J.M., Rohrbeck, L., Rausch, L., Sedimbi, S.K., Karlsson, M.C.I., Lambrecht, B.N., Karlsson Hedestam, G.B., et al. (2017). PPAR-gamma promotes type 2 immune responses in allergy and nematode infection. Sci. Immunol. *2*, eaal5196. https://doi.org/10.1126/sciimmunol.aal5196.

58. Batyrova, B., Luwaert, F., Maravelia, P., Miyabayashi, Y., Vashist, N., Stark, J.M., Soori, S.Y., Tibbitt, C.A., Riese, P., Coquet, J.M., and Chambers, B.J. (2020). PD-1 expression affects cytokine production by ILC2 and is influenced by peroxisome proliferator-activated receptor-gamma. Immun. Inflamm. Dis. *8*, 8–23. https://doi.org/10.1002/iid3.279.

59. Liu, Q., Dwyer, G.K., Zhao, Y., Li, H., Mathews, L.R., Chakka, A.B., Chandran, U.R., Demetris, J.A., Alcorn, J.F., Robinson, K.M., et al. (2019). IL-33-mediated IL-13 secretion by ST2+ Tregs controls inflammation after lung injury. JCI Insight *4*, e123919. https://doi.org/10.1172/jci.insight.123919.

60. Lee, M.W., Odegaard, J.I., Mukundan, L., Qiu, Y., Molofsky, A.B., Nussbaum, J.C., Yun, K., Locksley, R.M., and Chawla, A. (2015). Activated type 2 innate lymphoid cells regulate beige fat biogenesis. Cell *160*, 74–87. https://doi.org/10.1016/j.cell.2014.12.011.

61. Collazo, M.M., Paraiso, K.H.T., Park, M.Y., Hazen, A.L., and Kerr, W.G. (2012). Lineage extrinsic and intrinsic control of immunoregulatory cell numbers by SHIP. Eur. J. Immunol. *42*, 1785–1795. https://doi.org/10.1002/eji.201142092.

62. Dubois, E., Jacoby, M., Blockmans, M., Pernot, E., Schiffmann, S.N., Foukas, L.C., Henquin, J.C., Vanhaesebroeck, B., Erneux, C., and Schurmans, S.. (2012). Developmental defects and rescue from glucose intolerance of a catalytically-inactive novel Ship2 mutant mouse. Cell Signal. *24*, 1971–1980.

STAR★METHODS

KEY RESOURCES TABLE

REAGENT or RESOURCE	SOURCE	IDENTIFIER
Antibodies		
See Table S1 Antibodies		
Chemicals, peptides, and recombinant proteins		
K118	Brooks et al.,2015[37]	N/A
K149	Hoekstra et al., 2016[45]	N/A
K161	Pedicone et al., 2020[40]	N/A
3AC	Brooks et al.,2010[36]	N/A
As1949490	Tocris Biosciences	Cat# 3718
Klucel (Hydroxypropylcellulose, M.W.60,000)	Sigma-Aldrich	Cat# S452343
Collagenase II	Sigma-Aldrich	Cat# C6885
RBC lysis buffer, eBioscience™ 10X RBC Lysis Buffer (Multi-species)	ThermoFisher Scientific	Cat# 00-4300-54
Zombie Aqua Fixable Viability Kit	Biolegend	Cat #423102
eBioscience IC Fixation Buffer	ThermoFisher Scientific	Cat# 00-8222-49
eBioscience Permeabilization Buffer (10X)	ThermoFisher Scientific	Cat# 00-8333-56
Critical commercial assays		
Mouse IL-5 DuoSet ELISA	R&D Systems	Cat# DY405
Experimental models: Cell lines		
Mouse BV2 Inpp5d clone 2 (BV2 clone 2)	Pedicone et al., 2022	N/A
Experimental models: Organisms/strains		
C57BL/6J	Jackson Laboratory	Stock No. 000664
B6.129S6-Inpp5dtm1Wgk/J (SHIP1$^{flox/flox}$)	Jackson Laboratory	Stock No. 028255
B6.SJL-$Ptprc^a$ $Pepc^b$/BoyJ (B6.SJL)	Jackson Laboratory	Stock No. 002014
BALB/cJ (Balb)	Jackson Laboratory	Stock No. 000651
C.129S1(B6)-$Gata1^{tm6Sho}$/J, (ΔdblGATA)	Jackson Laboratory	Stock No. 005653
B6.129P2-$Lyz2^{tm1(cre)lfo}$/J (LysMCre)	Jackson Laboratory	Stock No. 004781
EoCre	Doyle et al., 2013[56]	N/A
SHIP2$flox/flox$	Dubois et al., 2012[62]	N/A
Software and algorithms		
FlowJo v9.9.6–10.8.1	BD Biosciences	https://www.flowjo.com
SpectroFlo Version 2.2.0.2		https://cytekbio.com/pages/aurora
Prism 9–9.4.1	GraphPad	https://www.graphpad.com/
BioTek Gen2 Data analysis software	Agilent	https://www.biotek.com/
PIXImus2 densitometer Software version 2.10	GE Medical systems	http://www.piximus.com/
Other		
Microvette® 100 Serum, 300 μL	Sarstedt	Cat#20.1308.100
High Fat Diet (HFD), Rodent Diet With 60 kcal% Fat	Research Diets	Cat#D12492
Accu-Chek Guide Glucose Meter	Roche Diagnostics	

RESOURCE AVAILABILITY

Lead contact

Further information and requests for resources and reagents should be directed to and will be fulfilled by the Lead Contact: William G, Kerr, Ph.D., Professor of Microbiology & Immunology, wgkerr@mac.com, SUNY Upstate Medical University, 750. E. Adams Street, WH2204, Syracuse, NY 13210.

Materials availability

Mouse lines used in this study have been deposited at Jackson Laboratories (SHIP1^{flox}(Stock No. 004781), LysMCre, ΔdblGATA) or can be obtained from Stéphane Schurmans, Ph.D. (SHIP2^{flox}; sschurmans@uliege.be) or Elizabeth Jacobsen, Ph.D. (eoCre; Jacobsen.Elizabeth@mayo.edu).

The SHIP1/2 inhibitory compounds used in this study can be obtained from commercial sources, Echelon Biosciences: 3AC, K118, K149 or Tocris Pharmaceuticals: AS1949490. K161 can be provided upon request; however, this requires its chemical synthesis and purification and thus it's availability will be dependent upon the willingness of the requestor to provide financial support for its production.

SHIP1-deficient BV2 microglial cells (clone C2) can be obtained from the lead contact or Rosa Chiara Paolicelli, Ph.D., University of Lausanne (rosachiara.paolicelli@unil.ch).

Data and code availability

There is no code described in this paper. All data reported in this paper will be shared by the lead contact-upon request. Any additional information required to evaluate our findings or to obtain materials described herein can be requested from the lead contact and he will, to the best of his ability, provide this information in a timely fashion if it is feasible to do so.

EXPERIMENTAL MODEL AND SUBJECT DETAILS

Mice

C57BL6/J (Stock No.:000664), B6.SJL (Stock No.:002014), Balb/c (Stock No.:000651) and ΔdblGATA (Stock No.: 005653) mice were purchased from Jackson Labs. SHIP1$^{flox/flox}$ were generated in the lab and deposited at Jackson Labs (Stock No. 028255). EoCre mice were generously provided by Elizabeth A Jacobsen, Ph.D., Mayo Clinic Arizona. LysMCreSHIP1$^{flox/flox}$ mice were generated in the lab by crossing LysMCre (B6.129P2-*Lyz2*$^{tm1(cre)lfo}$/J, Jackson Labs Stock No. 004781) mice to SHIP1$^{flox/flox}$ mice as previously described. LysMCreSHIP2^{floxflox} and LysMCreSHIP1$^{flox/flox}$SHIP2$^{flox/flox}$ were generated by crossing LysMCreSHIP1$^{flox/flox}$ to SHIP2^{floxflox} mice. EoCreSHIP1$^{flox/flox}$, eoCreSHIP2$^{flox/flox}$ eoCreSHIP1$^{flox/flox}$SHIP2$^{flox/flox}$ were obtained by crossing eoCre mice with SHIP1$^{flox/flox}$, SHIP2$^{flox/flox}$ and SHIP1$^{flox/flox}$SHIP2$^{flox/flox}$, respectively. Mice were fed a high fat (60 kcal) % diet (HFD, Research Diets D12492) *ad libitum* starting at 6 weeks of age and were maintained on this diet for the duration of the study. For the prevention studies, mice were treated with SHIPi starting on day 1 of HFD. For the obesity reversal studies, mice were placed on HFD for 8 weeks prior to initiating the SHIPi treatment. ILC2 data was generated using aged B6.SJL mice on a normal mouse chow diet. The SUNY Upstate Medical University IACUC approved all animal experiments.

SHIP inhibitor treatment of mice

K118 and K161 were dissolved in water and delivered at 10mg/kg in 10 μL/g. AS1949490 (Tocris Bioscience) and K149 were initially dissolved in 100% DMSO and diluted to 5% with normal saline (0.9%w/v) and administered at 20 mg/kg and 10 mg/kg, respectively. 3AC was emulsified in 0.3% Klucel (hydroxypropylcellulose M.W. 60,000, Sigma Aldrich): saline (w/v) and administered at 26.5 mg/kg. The vehicle groups were H$_2$O (10 μL/g) for K118 and K161, 5% DMSO: saline (10 μL/g) for AS1949490 and K149, or 0.3% Klucel:saline (20 μL/g) for 3AC. Mice were injected intraperitoneally with a syringe fitted with a 29-gauge needle with the compounds or vehicle twice a week for two to six weeks as indicated in the respective figures.

Detection of immune cells in adipose tissue by flow cytometry

Perigonadal white adipose tissue (WAT) was removed from mouse following euthanasia via CO$_2$ inhalation and perfusion with 20 mL cold perfusion buffer (0.5% BSA in 1X PBS, sterile filtered). WAT was minced in 3 mL cold perfusion buffer and transferred to 50 mL conical tubes and kept on ice. 3 mL of Collagenase

II buffer (Collagenase II 4 mg/mL; Sigma Aldrich, 10 mM CaCl2 in Perfusion buffer) was then added and samples were digested for 20 minat 37°C with shaking at 200 rpm. Digested tissue was triturated with 10 mL cold perfusion buffer and sheared through a 100 μm filter into a clean 50 mL conical tube. Samples were centrifuged at 500xg for 10 minat 4°C, floating adipocytes were removed by aspiration and the pellet containing stromal vascular fraction (SVF) was resuspended in 2 mL of 1X RBC lysis buffer (Thermo Fisher Scientific) and placed on ice for 5 min. Samples were diluted with 18 mL cold 1X PBS, filtered through a 70 μm strainer and centrifuged at 400xg for 5 minat 4°C. After decanting supernatant, the cell pellet was resuspended in 5 mL, cells were counted distributed in round bottom tubes and samples were washed (2 mL cold 1X PBS, centrifuged at 400xg for 5 minat 4°C, and supernatant was decanted). Samples were stained with Zombie Aqua Live/Dead (Biolegend) for 20 min on ice in 100 μL to allow for dead cell exclusion. Cells were washed as above and Fc blocked (TruStain FcX (anti-mouse CD16/32) antibody, Biolegend) in 50 μL of Flow Buffer (3% Heat-Inactivated Serum, 10 mM Hepes in 1X PBS, sterile filtered) followed by surface staining in 50 μL with antibody cocktails listed below for 30 min on ice. Cells were then washed as above. For intracellular staining following surface stains, cells first fixed by resuspending in 200 μL of IC Fixation Buffer (Thermo Fisher Scientific) for 20 min on ice and washed (2 mL 1X Permeabilization buffer (Thermo Fisher Scientific), centrifuged at 400xg for 5 minat 4°C, and supernatant was decanted). Cells were Fc blocked in 50 μL 1X Permeabilization buffer and stained with intracellular antibody cocktails in 50 μL 1X Permeabilization buffer on ice for 30 min, and washed twice as above. For SHIPi- and Veh treated WT mice, the eosinophil surface staining cocktail was: SiglecF-PE, CD45-PerCP/Cyanine5.5, CD11b-APC/Cyanine7, Gr1-BV605, CD11c-BV650 and intracellular staining with IL4-AlexaFluor488. For M1, M2 and MDSC, the surface staining cocktail for SHIPi- and Veh-treated WT and DeltadblGata mice was: anti-mouse F4/80-AlexaFluor488, CD19 PerCP/Cyanine 5.5, CD11c-PE/Cyanine7, CD11b-APC/Cyanine7, Gr1-BV605 and CD86-PE or CD86-BV785. In LysMCreSHIP1$^{flox/flox}$SHIP2$^{flox/flox}$ mice, surface staining cocktail for eosinophils was as above for WT mice followed by intracellular staining with SHIP1-AlexaFluor647. In EoCreSHIP1$^{flox/flox}$SHIP2$^{flox/flox}$ mice, eosinophil stain was SiglecF-AlexaFluor647, CD45-PerCP/Cyanine5.5, CD11b-APC/Cyanine7, Gr1-BV605, CD11c-BV650 and intracellular staining with SHIP1-PE. Following final washed samples were acquired on a BD Fortessa flow cytometer (BD Biosciences) and data were analyzed using FlowJo software versions 9.9.6–10.8.1(BD Biosciences). For the ILC2 staining, cells were isolated from WAT of aged WT mice treated with K161 or Veh as above, and stained with Zombie Aqua Live/Dead (Biolegend) for dead cell exclusion, washing and blocking of Fc receptors and surface staining as described above. The ILC2 surface antibody cocktail sued was: anti-mouse Lineage-PerCP/Cyanine5.5, CD170 (SiglecF)-SuperBright436, IL33R (ST2)-AlexaFluor488, Sca1-PE/Cyanine5, CD127-AlexaFluor700, c-Kit-APC/AlexaFluor780, Gr1-BV605, CD11c-BV650, CD11b-BV711 and CD45-PerCP and followed by intracellular staining with IL13-PE. Samples were acquired on the Cytex Aurora with SpectroFlo 2.0 software, and further analyzed using FlowJo software 10.6–10.8.1.

Treatment of C2 cells with SHIP inhibitors

BV2 clone 2 cells (C2 cells) were grown in DMEM:F12 media supplemented with 10% Heat Inactivated fetal bovine serum. After harvesting, cells were distributed in falcon tubes at 0.5M/ml in 0.5mL/tube. Cells were washed with 2 mL PBS and centrifuged for 10 min at 250 x g at room temperature. Supernatants were decanted and cells were resuspended in 0.5 mL warm growth media containing K149 (5 μM in 0.5% DMSO: media), K161 (5 μM in 0.5%H_2O:media, DMSO (0.5%DMSO:Media) or H_2O (0.5% H_2O:media) and incubated for 30 min at 37°C with 5%CO_2. 2 mL of ice-cold PBS was added to each tube, samples were centrifuged 10 min at 250 x g at 4°C, decanted and kept on ice. Samples were stained with Zombie Aqua Live/Dead (Biolegend) for 20 min on ice in 100 μL to allow for dead cell exclusion, followed by washing as above. Cells were then fixed by resuspending in 200 μL of IC Fixation Buffer (Thermo Fisher Scientific) for 20 min on ice and washed (2 mL 1X Permeabilization buffer (Thermo Fisher Scientific), centrifuged at 400xg for 5 minat 4°C, and supernatant was decanted). Cells were Fc blocked in 50 μL 1X Permeabilization buffer and stained with intracellular antibody cocktail (anti-Akt pS473_AlexaFluor488, Phospho-mTor (Ser2448)_PE-Cy7)) in 50 μL 1X Permeabilization buffer on ice for 30 min, and washed twice as above. Samples were acquired on the Cytex Aurora with SpectroFlo 2.0 software, and further analyzed using FlowJo software 10.8.1.

Blood glucose

Blood glucose was measured in whole blood from tail vein snip using a blood glucometer (Accu-Chek Guide, Roche Diagnostics), 16 h after the final dose of SHIPi or Veh.

IL5 ELISA

Blood was collected by facial vein puncture using a 25-gauge needle into serum collection tubes (Sarstedt Microvette 300Z). Serum was isolated from whole blood following 10' centrifugation at 10,000xg at room temperature, and stored at −20°C until use. ELISA was performed using Mouse IL-5 Duo Set (R&D Systems) according to manufacturer's recommendations.

DEXA analysis

Body composition was measured pre and post treatment with a PIXImus2 densitometer (GE, Madison, WI), and analyzed with software version 2.10. Mice were anesthetized with isoflurane (Forane, USP, Baxter Healthcare Corporation, IL) throughout body scan.

QUANTIFICATION AND STATISTICAL ANALYSIS

All statistical analyses were performed using the statistical softwarePrism 8.4–9.4.1 (GraphPad, San Diego, CA), as described in the legend to each figure.